Use Of Synthetic Solid Scaffolds To Mechanically Support A Chondrocyte-Seeded Peptide Hydrogel For Articular Cartilage Repair

by

Jennifer R. Ibañez

S. B. Biological Engineering
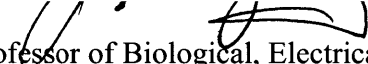Massachusetts Institute of Technology, 2016

Submitted to the Department of Biological Engineering in Partial
Fulfillment of the Requirements for the Degree of

Master of Engineering in Biomedical Engineering
at the
MASSACHUSETTS INSTITUTE OF TECHNOLOGY

June 2017

Signature of Author...................
Signature redacted
....
Department of Biological Engineering
May 12, 2017

Certified By...................
Signature redacted
....
Alan J. Grodzinsky
Professor of Biological, Electrical, and Mechanical Engineering
Thesis Supervisor

Accepted By.......................
Signature redacted
....
Mark Bathe
Associate Professor of Biological Engineering
Chairman, Graduate Program Committee
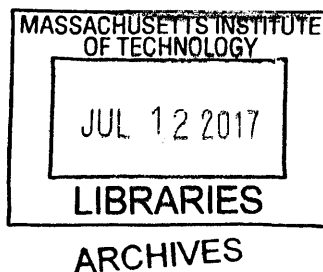
1

Use Of Synthetic Solid Scaffolds To Mechanically Support A Chondrocyte-Seeded Peptide Hydrogel For Articular Cartilage Repair

by

Jennifer R. Ibañez

Submitted to the Department of Biological Engineering
on May 12, 2017 in Partial Fulfillment of the
Requirements for the Degree of Master of Engineering in
Biomedical Engineering

Abstract

Post-traumatic osteoarthritis (PTOA) is a subtype of OA associated with cartilage defects caused by traumatic joint injury. Because articular cartilage has a limited innate healing response, due to its avascular, aneural, and alymphatic nature, these defects lead to chronic degenerative joint disease if left untreated. Current treatments to repair articular cartilage generally result in fibrocartilage that is mechanically and biochemically inferior to native hyaline tissue. This has motivated the development of tissue engineering strategies for cartilage defect repair. Hydrogel approaches have shown promising results in their ability to induce chondrogenesis, proliferation, and cartilage-like matrix production, but are often very soft at early time points and at risk of damage from joint articulation. Solid scaffolds solve this mechanical problem, but often sacrifice bioactivity and integration with native tissue. In order to avoid the drawbacks of each of these approaches, we proposed a composite scaffold approach using a synthetic solid scaffold, made of bioabsorbable polyglycolic acid:trimethylene carbonate (PGA:TMC) or expanded polytetrafluoroethylene (ePTFE), loaded with a chondrocyte-seeded self-assembling peptide hydrogel, [KLDL]$_3$. We hypothesized that these composite scaffolds would benefit from the mechanical protection of the solid scaffolds as well as the pro-chondrogenic and proliferative effects of the KLD hydrogel, allowing chondrocytes to produce cartilage-like extracellular matrix in a protected mechanical environment. To test the potential of these composite scaffolds for use in cartilage repair, we measured cell distribution, viability, matrix production and accumulation, and static and dynamic mechanical properties. We found that cells could be evenly distributed through at least one of the solid scaffolds tested, with all showing proliferation and maintenance of viability over four-week culture. Per-cell matrix production was an order of magnitude higher than in KLD hydrogels alone. Mechanical properties of composite scaffolds appeared to be dominated by the solid scaffolds, showing that they offered mechanical protection to the soft hydrogel within. Use in a cartilage defect model showed potential for integration with native tissue given optimization of gel-casting methods. Overall, our results show that these composite scaffolds are a viable tissue engineering strategy for articular cartilage repair.

Thesis Supervisor: Alan J. Grodzinsky
Title: Professor of Biological, Electrical, and Mechanical Engineering

Acknowledgements

This past year and a half has been a whirlwind of a journey, and I am both sad to see it end and excited to see what the next chapter of my life brings. There are so many people who have made this work possible, and one page isn't nearly enough to say thank you to everyone—but I'll try, anyway.

Thank you to Professor Al Grodzinsky, for being a better advisor and mentor than I could have hoped for. Your constant optimism and positivity always kept me motivated and excited about my research, and your joyful personality made all of our group meetings and lab events so much fun. You have taught me so much in the last year about cartilage, about being a researcher, and about being a great human being. I'll let you know when I get my Tesla.

Thank you to all the members of the Grodzinsky lab, for being amazing lab-mates and friends. To Hannah, for all of your help in the lab, always being someone to bounce ideas off of, and being a great friend and desk-mate to talk to and eat cheese with. To Paul, for all of your guidance and for helping me tackle my nemesis, statistics. To Han-Hwa, for single-handedly making sure that the lab didn't fall apart and for all of your wisdom on anything I ever needed to know about running my experiments. To Eliot, for making the Dynastat data seem so simple. And to Bri, Yang, Yamini, Linda, John, Whitney, Ramin, Brett, and all of the UROP squad, for making my time in the lab an absolute blast. Margarita Fridays and Area Four pizzas won't be the same without you.

Most importantly, thank you to my family and friends for your constant love and support. To my parents, Amy and Rodrigo, for encouraging my love of science from the beginning and for your unwavering enthusiasm for everything I do. I can always count on you to think my microscope images look amazing or that even my most meager experiment results are going to change the world. To my boyfriend Henry, for always letting me complain to you about lab things you don't understand, bringing me food and cheering me up on late lab nights, and just generally being the best. And to my dog, Koda, for loving me unconditionally and making goofy faces that my parents send me pictures of. I love all of you so, so much.

Table of Contents

List of Figures

1. Introduction

3. Results

4. Discussion

1. Introduction

1.1 Structure and mechanics of articular cartilage

Articular cartilage is an avascular, aneural, and alymphatic tissue with a limited innate healing response. It consists of a single cell type, chondrocytes, comprising only about 2 – 5% of the tissue by volume. The majority of the tissue is dense extracellular matrix composed of collagen and proteoglycans. Collagen fibrils make up about 25% of the tissue by wet weight, providing tensile strength and a structural network for the tissue.[1] Because this tissue is hyaline cartilage, the collagen fibrils contain primarily type II (along with types IX and XI), contrary to the type I collagen fibrils that dominate fibrocartilage and other connective tissues, including tendons, ligaments and bone. The half-life of collagen in articular cartilage is ~120 years, meaning that there is very little turnover of collagen in the tissue during adulthood.[2]

The gaps between collagen fibrils are filled with a hydrogel of proteoglycans, the majority of which are aggrecan molecules that consist of a protein core and ~100 sulfated glycosaminoglycan (sGAG) chains in a bottlebrush structure.[3] In contrast to collagen, the half-life of aggrecan proteoglycans in articular cartilage is about 3 years.[4] The high water content of this "gel" confers poroelastic behavior to the tissue. When mechanical load is applied to the tissue, water is forced out of the various zones of cartilage into the surrounding synovial space. The water re-enters the tissue when the load is removed. This behavior allows articular cartilage to withstand greater loading, especially at higher loading rates.[5] Surrounding each chondrocyte is a thin layer of pericellular matrix (PCM), which protects the cells from mechanical stresses and plays a role in mechanotransduction. The PCM is comprised of a dense network of proteoglycans, fibronectin, and collagen type VI.[6, 7]

The primary function of chondrocytes in mature cartilage is to secrete ECM proteins in order to maintain the appropriate mechanical properties for the tissue. Because the turnover of many of these proteins is relatively slow, the anabolic and proliferative activity of chondrocytes under normal conditions in healthy cartilage is low compared to many other cell types. Due to avascularity of the cartilage, any nutrients or growth factors required by the cells must diffuse

into the tissue from the synovial fluid or, under special circumstances, from the subchondral bone.[8] The structure of articular cartilage makes innate repair of defects challenging, motivating the development of tissue engineering and regenerative approaches.

1.2 Osteoarthritis and articular cartilage defects

Osteoarthritis is a complex disease with many subtypes, one of which is post-traumatic osteoarthritis (PTOA). PTOA is associated with cartilage defects caused by traumatic joint injury and, if untreated, will lead to chronic degenerative joint disease. The cell scarcity and absence of vasculature in cartilage lead to a weak innate healing response for these injury-induced defects, and make it difficult to treat the disease without surgical intervention. The body does very little to repair partial thickness cartilage defects, and these will likely persist until they progress to full thickness defects through further wear and degeneration.[9] Full thickness defects elicit a greater healing response, triggering migration of marrow-derived cells from subchondral bone and generally leading to production of fibrocartilage. However, this new fibrous cartilage is mechanically inferior to the native hyaline cartilage it attempts to replace, and integrates poorly with the existing tissue.[10, 11] The body is thus unable to adequately repair cartilage defects on its own, and tissue engineering or regenerative approaches must be taken to prevent pain and further tissue damage.

1.3 Commonly used methods for cartilage repair

1.3.1 Marrow stimulation techniques

Marrow stimulation techniques, including microfracture, drilling, and debridement, rely on removing the calcified zone of articular cartilage in order to access the underlying subchondral bone. Debridement involves cleaning up rough edges around the defect by excising damaged cartilage fragments and removing the calcified region. This is thought to allow synthesis of new tissue at the base of the defect and improve integration of repair tissue with the healthy cartilage. Additionally, removal of damaged tissue fragments may reduce secretion of matrix metalloproteinases that further degrade surrounding cartilage and worsen the defect. Results have

been varied, with most positive results deteriorating within five years of surgery, and the method remains in dispute among orthopedic surgeons.[12–14]

In microfracture, an arthroscopic awl is used to puncture 3 – 4 mm holes into the subchondral bone in order to promote stem cell migration from the bone marrow into the defect. This is an improvement over making these holes via surgical drilling, as it solves the issue of overheating the surrounding tissue during the drilling procedure. Although repair tissue is formed following microfracture, it is fibrocartilage rather than hyaline cartilage and, as stated above, is mechanically inferior to and biochemically distinct from the native cartilage tissue.[15] This fibrous repair tissue often deteriorates within a few years after surgery, and intra-lesional osteophytes are fairly common, developing in 20 – 50% of cases.[15, 16]

1.3.2 Autologous chondrocyte implantation (ACI)

ACI is a two-surgery procedure. In the first surgery, healthy cartilage biopsies are harvested from the patient. Chondrocytes are isolated from this tissue, passaged three times and expanded *in vitro*, and then injected into the cartilage defect during the second surgery three to four weeks later. By the time of injection, after three passages, it is known that the cells have de-differentiated into a fibroblastic, or non-chondrogenic phenotype.[17] This means that upon injection, they would have to re-differentiate in order to synthesize cartilage-specific matrix molecules. The cells are typically kept in place with a periosteal patch, which is taken from the proximal medial tibia of the joint during the second procedure.[18] A significant disadvantage of this approach is the requirement for two invasive surgical procedures, along with potential for donor site morbidity where the initial cartilage is harvested.[19] Results have also been mixed, with some histological studies showing repair tissue that is inferior to native hyaline cartilage.[20] Another potential drawback with ACI is that chondrocytes could be settling to the bottom of the defect, rather than being distributed throughout the entire volume of the defect. This could lead to uneven formation of repair tissue and poor integration with the native tissue. To combat this problem, matrix-induced autologous chondrocyte implantation (MACI) was developed in which the patient's chondrocytes from the first surgery are seeded on the surface of

a matrix, such as a collagen scaffold, which is then used to fill the volume of the defect. This method has achieved marginally better results than ACI alone.[21, 22]

1.4 Use of hydrogels for articular cartilage repair

A wide variety of synthetic and natural polymer-based hydrogels have been investigated for use in articular cartilage repair. These offer many logistical benefits, such as uniform cell distribution, in-situ gelation that allows conformation to defect morphology, and high water content that mimics *in vivo* ECM conditions, among others. Injectable hydrogels also allow for minimally invasive surgical procedures. However, they do have shortcomings, such as low mechanical strength. A select few hydrogel scaffold materials will be discussed here.

1.4.1 Agarose

Agarose was one of the first biomaterial-based hydrogels to be used for articular cartilage repair, and it has been shown to support chondrogenesis and the production of GAGs.[17, 23] Chondrocyte-seeded gels were also able to reach Young's moduli comparable to native cartilage in a canine model, showing potential to mimic biomechanical properties of the native tissue after several weeks in culture.[24] This mechanical functionality at long time points was consistent with other previous *in vitro* studies.[25] At early time points before chondrocytes have synthesized new matrix, mechanical strength of agarose gels is low.[26] Another drawback of agarose is its slow and unpredictable biodegradation, during which time large byproducts may be released and elicit a macrophage response.[27] Additionally, chondrocytes do not adhere to agarose scaffolds, so the gels must be functionalized with RGD or other binding peptides in order to promote cell adhesion during early time points when minimal ECM has been produced.[28] It is possible, however, that these conjugated proteins could inhibit chondrogenesis.[29]

1.4.2 Alginate

Alginate is another polysaccharide polymer scaffold similar to agarose, with many of the same advantages and disadvantages for use in cartilage repair. It is typically cross-linked via calcium ions, although many studies use ion concentrations much lower than physiological levels, leading to higher cross-linking density when experiments are moved *in vivo*.[30] Alginate gels have been shown to maintain chondrogenic phenotype, including production of matrix proteins [31], and to enable fundamental studies of the effects of mechanical loading on chondrocyte biosynthesis and turnover.[32] However, the same issues exist for cartilage repair as with agarose gels, namely the low mechanical strength, potential for foreign body giant cell response, and inability for cells to adhere to the scaffold alone. [28, 33]

1.4.3 Self-assembling peptides

Self-assembling peptides are an emerging class of biomaterial-based hydrogels for cartilage repair, offering benefits over traditionally used materials and showing promising results *in vitro* and *in vivo*.[34] Synthetically produced self-assembling peptides avoid the risk of pathogenicity inherent to natural or animal-derived biomaterials.[35] The peptides discussed here, specifically [KLDL]$_3$ and [RADA]$_4$, are those with alternating hydrophilic and hydrophobic side chains, which allow them to assemble into a hydrogel network without the need of a crosslinking agent (Figure 1). The polymers form β-sheets, which then assemble into a membranous network of interwoven fibers under physiologic pH and ionic strength.[36] Their assembly under these conditions makes them well suited for injection directly into cartilage defects. The chemistry of these hydrogels also allows for growth factors or other drugs to be adsorbed or tethered to the scaffold for delivery, expanding their potential applications and benefits in cartilage repair.[37] Studies have found that [KLDL]$_3$ and [RADA]$_4$ hydrogels promote chondrogenesis of bone-marrow progenitor cells, enhance matrix production and proliferation in chondrocytes, and are able to improve cartilage repair *in vivo*.[38–40] A negative of these gels, similar to the agarose and alginate hydrogels discussed above, is their low mechanical strength at early time points.[39] While this softness facilitates stem cell migration and may contribute to their chondrogenic effects, it also makes the gels susceptible to damage from joint articulation in the early weeks following surgery.

1.5 Use of solid scaffolds for cartilage repair

Solid scaffolds, primarily made with synthetic polymers, have also been investigated for use in cartilage repair. Commonly used materials include poly-caprolactone (PCL), poly (glycolic acid) (PGA), and poly (lactic acid) (PLA), among others. These materials exhibit greater mechanical strength, protecting any developing neocartilage from mechanical damage during early time points, but have shown poor bioactivity and integration in comparison to hydrogel scaffolds.[41] Composite scaffold approaches have been taken to increase bioactivity and cell adhesion.[42] Polyester-based solid scaffolds may also elicit a foreign body giant cell response as they degrade, and may increase local acidity and pH if the degradation products are not biocompatible.[43, 44]

1.6 Hydrogels and solid scaffolds used in combination

In order to overcome the individual shortcomings of both hydrogels and solid scaffolds, studies have investigated the combination of the two. The hypothesis is that the hydrogel will maintain its pro-chondrogenic and matrix production effects, with the added mechanical integrity of the solid scaffold providing protection at early time points while neocartilage is still forming. Using hydrogels as a cell-carrier within solid scaffolds also ensures more even cell distribution. In a study using chondrocyte-seeded alginate hydrogels within polyglactin (PLGA) scaffolds compared to the PLGA scaffolds alone, the hydrogel was found to maintain even cell distribution and prevent the solid scaffold from contracting and warping.[45] Although the matrix production was the same in both conditions, the alginate embedded scaffold would have better integration and well distributed repair tissue production throughout the volume of the defect.

The hydrogel component of composite scaffolds is more than just a method of evenly distributing cells, though. As discussed above, many hydrogels studied for cartilage repair have chondrogenic effects and promote matrix production. A study comparing PGA scaffolds loaded with mesenchymal stem cells (MSCs) in either alginate or collagen type I hydrogels found varying levels of GAG production and chondrogenesis between the two.[46] Another study investigated a composite scaffold consisting of a 3D PCL scaffold loaded with chondrocyte-seeded RAD hydrogels. The presence of the RAD hydrogel was essential for chondrogenic gene

expression, while the presence of the PCL scaffold provided mechanical stability at early time points and prevented the RAD hydrogel from contracting and compacting over the four-week culture.[47]

1.7 Thesis objectives and summary of results

The objective of this work was to create a composite scaffold from 3D synthetic solid scaffold materials and chondrocyte-seeded KLD hydrogels as a strategy for cartilage repair. Two different types of solid synthetic scaffolds were used in this study, bioabsorbable polyglycolic acid:trimethylene carbonate (PGA:TMC) and expanded polytetrafluoroethylene (ePTFE). Several variants of each were initially tested for wettability and thickness before the field was narrowed down for use in cell matrix biosynthesis, biochemical and mechanical studies. Two variants of each material were used; variants of bioabsorbable PGA:TMC will henceforth be referred to as P:T-1 and P:T-2, while variants of ePTFE will be referred to as ePTFE-1 and ePTFE-2. KLD, a self-assembling peptide described in section 1.4.3 above, was chosen for its promotion of chondrogenesis, matrix production, and cell proliferation. Variations of PGA/TMC and ePTFE have been used in other implantable medical devices, and have been shown to support chondrocyte growth.[48, 49]

The specific aims of this work were to:

1. Evaluate the ability of bioabsorbable PGA:TMC and ePTFE constructs to allow penetration and *in situ* gelation of self-assembling KLD peptide, with and without chondrocytes mixed into the KLD solution.

2. Quantify viability of chondrocytes during long-term (four-week) culture in composite scaffolds.

3. Demonstrate that chondrocytes in composite scaffolds can synthesize new cartilage-like matrix, specifically through analyzing the production of sGAG during long-term culture.

4. Measure the static and dynamic compressive stiffness of cell-seeded composite scaffolds during long-term culture.

Results of this work demonstrated that the composite scaffolds supported cartilage-like matrix production at higher per-cell levels than in KLD-hydrogels alone. The PGA:TMC scaffolds were also able to provide mechanical strength at early time points, as the mechanical behavior of these materials dominated mechanical behavior of the composite scaffolds over the four-week culture. A pilot study of integration of repair tissue with native tissue in a cartilage defect model over two weeks demonstrated the potential for good integration of the composite scaffold repair tissue with native cartilage. Matrix production rates and accumulation of matrix in this pilot study was similar to levels in the composite scaffolds alone, and a small number of cells were able to migrate from the composite scaffold into the native tissue.
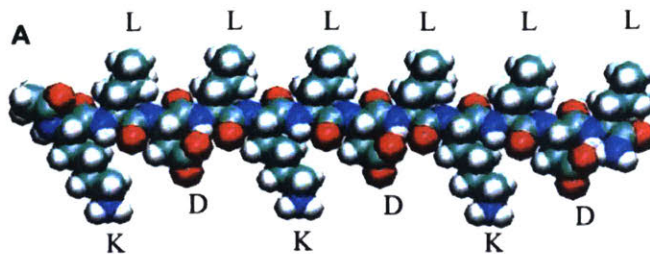
Figure 1.1: Structure of [KLDL]₃ peptide. Alternating hydrophilic and hydrophobic side chains are shown. Hydrophobic leucines (L) alternate with hydrophilic positively charged lysines (K) and negatively charged aspartic acids (D) to form β-sheets. Figure adapted from [39].

2. Methods

2.1 Chondrocyte and cartilage plug harvest

Chondrocytes were harvested from the medial and lateral femoral condyle and trochlear groove of 1 – 2 week old bovine calf knee joints (Research 87, Inc. Boylston, MA). Pieces of articular cartilage were shaved from the surfaces using a scalpel and chopped into smaller fragments to improve digestion before being transferred to a spinner flask with 2 mg/mL proteinase (Sigma-Aldrich, St. Louis, MO) in chondrocyte isolation medium, which was baseline medium plus 10% fetal bovine serum (FBS)(GE Healthcare Life Sciences, Hyclone Labs, Logan UT). Baseline medium for experiments consisted of low-glucose Dulbecco's modified Eagle's medium (DMEM) (Mediatech Inc., Manassas, VA), 100 U/mL penicillin, 100 μg/mL streptomycin, and 0.25 μg/mL amphotericin (PSA) (Invitrogen, Carlsbad, CA), 10mM 4-(2-hydroxyethyl)- 1-piperzaineethanesulfronic acid (HEPES)(Invitrogen), 0.1 mM non-essential amino acids (NEAA)(Sigma-Aldrich), 0.4 mM proline (Sigma-Aldrich), and 37.5 μg/mL ascorbate-2-phosphate (Wake Chemicals, Richmond, VA). Tissue was incubated in the proteinase for 1.5 – 2 hours at 37°C and 5% CO_2, then rinsed twice with sterile 1X phosphate-buffered saline (PBS)(Sigma-Aldrich) before 0.25 mg/mL collagenase (Sigma-Aldrich) in chondrocyte isolation medium was added. Cells were incubated overnight at 37°C.

The following morning, cells were pipetted 10 – 15 times to mechanically disrupt any remaining undigested tissue. The resulting cell suspension was filtered through a 70 μm pore strainer followed by a 40 μm pore strainer and then spun down in a centrifuge for 8 minutes at 1000 g. Cells were resuspended and rinsed with PBS, spun down again, resuspended and rinsed with PBS a second time, spun down once more, and finally resuspended in culture medium to be counted and used in casting experiments. Culture medium consisted of baseline media with 0.2% FBS and 1% ITS Premix (insulin-transferrin-selenium, 10 μg/ml, 5.5 μg/ml and 5 ng/ml, respectively, BD Biosciences, San Jose, CA) based on previous studies.[50]

Cartilage plugs of 6mm diameter were taken from the trochlear groove of the same joints described above. The first 0.7 mm of superficial zone was removed from the surface of the

15

plugs. Middle zone tissue was then sliced to 1.4 mm thickness and a 4 mm plug was taken out of the middle to create cartilage rings with a 6mm outer diameter and 4 mm inner diameter. Rings were equilibrated in culture medium at 37°C overnight.

2.2 Casting cell-seeded gels into solid scaffold materials

Plugs of solid scaffold materials were punched using a 10 mm biopsy punch and placed in a 24-well plate. Plugs were then wet with 10% sucrose with 2.5 mM HEPES using a Büchner flask and funnel under vacuum. This allowed the material to more easily absorb the KLD hydrogel. Chondrocytes were spun down in a centrifuge for 5 minutes at 1000 g and resuspended in 10% sucrose with 2.5 mM HEPES. This cell solution was added to KLD peptide hydrogel, suspended in 10% sucrose, for a final concentration of 30 million cells/mL and 3.5 mg/mL KLD peptide. The sucrose/HEPES-soaked plugs were then pre-wet with 100 µL of KLD and cell solution using the Büchner flask and funnel under vacuum. This precautionary step ensured that the KLD and cell solution were distributed as evenly as possible throughout the volume of the plugs and displaced any remaining sucrose with HEPES from the initial vacuum wetting. Plugs were then placed back in the 24-well plate and an additional 50 µL of KLD and cell solution was pipetted onto the top. This created the final composite scaffold consisting of solid scaffold material loaded with chondrocyte-seeded KLD hydrogel. After a 2 – 5 minute period to allow this final volume to absorb into the plugs, 0.75 – 1 mL of assembly bath was slowly added to the wells to bring the solution to physiologic pH and ionic strength and cause gelation of the KLD. Assembly bath consisted of culture medium with 25 mM HEPES rather than 10 mM. An additional 0.75 – 1 mL of culture medium was added to each well before incubating at 37°C for the duration of the experiments. Media was changed every 2 – 3 days.

The above protocol was also used, with minor adjustments, for experiments in which chondrocyte-seeded composite scaffold plugs were placed within cartilage rings. Plugs of solid scaffold material were punched using a 4mm biopsy punch in order to fit within the inner diameter of the cartilage rings. The pre-wetting step was done using 16 µL of KLD and cell solution rather than 100 µL in order to adjust for the smaller dimensions of the plugs. The pre-wet plugs were then placed within the cartilage rings before adding 8 µL of KLD and cell

solution, rather than the 50 μL used above for the 10 mm plugs. All other steps were performed as described above.

2.3 Trypsin pretreatment of cartilage rings and dying of cells to visualize integration

Controlled depletion of GAG at the inner surface of the cartilage ring has been shown to improve integration of tissue-engineered constructs with the native tissue.[51] This was replicated in the cartilage ring experiments here via a trypsin pretreatment. 20 μL of 50 μg/mL trypsin (Sigma-Aldrich) was added to the center of the cartilage rings for 2 minutes at room temperature. After removing the trypsin, FBS was added for 2 minutes to neutralize any remaining enzyme. Rings were then washed with PBS.

In order to visualize integration of the composite scaffolds with the cartilage rings, the chondrocytes with which the scaffolds were seeded were dyed prior to seeding. Cells were dyed with carboxyfluorescein diacetate succinimidyl ester (CFSE) (Thermo Scientific, Logan, UT) according to a previously published protocol.[52] Samples were viewed with an Olympus FV 1000 confocal microscope.

2.4 Measuring matrix production by quantifying sGAG production

The rate of synthesis of sGAG was measured using radiolabel incorporation of ^{35}S-sulfate at weekly time points. For a given time point, ^{35}S-sulfate (Perkin Elmer, Waltham, MA) was added to culture medium at a concentration of 5 μCi/mL and samples were returned to the 37°C incubator for 1 – 2 days. An aliquot of culture medium with 5 μCi/mL of ^{35}S-sulfate was frozen at -20°C to use as a standard for that time point. Following the 1 – 2 day incubation period, samples were washed with radiolabel wash (45 μg/mL proline, 140 μg/mL sodium sulfate in PBS) (Sigma Aldrich) four times for 30 minutes at 4°C. Samples were centrifuged for 5 – 10 minutes at 1000 g in order to spin out all of the peptide hydrogel. 0.1 mg/mL Proteinase-K (Roche Applied Science, Indianapolis, IN) was added to digest the samples, which were then placed into a 60°C water bath for 1 – 2 days until no visible chunks of gel remained. Samples

were then frozen at -20°C and stored until radiolabel incorporation was measured. Total sGAG content was then measured via DMMB dye binding, as described previously.[53]

2.5 Measuring DNA content using PicoGreen

DNA content of Proteinase-K digested samples was measured using the Quant-iT PicoGreen dsDNA kit (Invitrogen) according to the manufacturer's protocol.[54]

2.6 Measuring static and dynamic mechanical behavior

Samples were measured in unconfined compression with a Dynastat mechanical spectrometer (IMASS, Hingham, MA) using a 20 mm diameter platen in a testing chamber with culture medium. A 60-second 2.5% displacement ramp was applied, followed by a 240-second hold to allow the stress to reach equilibrium. This ramp and hold was repeated a total of six times, for a total displacement of 15%. A 1% amplitude sinusoidal displacement was then applied at frequencies of 0.01, 0.02, 0.03, 0.05, 0.1, 0.2, 0.3, 0.5, and 1 Hz. The stress relaxation data for each ramp was fit with a decaying exponential in time ($A + B\,e^{-t/\tau}$) and the extrapolated final value (A) taken as the equilibrium stress. Equilibrium stress-strain data at 10%, 12.5%, and 15% strain were linear regression fit and the slope was taken as an estimate of the equilibrium stiffness. For sinusoidal data, the fundamental frequency components of the displacement and load signals were obtained using a discrete Fourier transform. These components were used to obtain the complex dynamic stiffness, which was split into magnitude and phase, with dynamic stiffness magnitude defined as the computed amplitude of the stress divided by strain amplitude.

2.7 Quantifying cell viability using alamarBlue

To quantify cell viability at a given time point, 1 mg/mL alamarBlue (Thermo Scientific) in culture medium was added to samples, which were then incubated at 37°C for 3 hours. Media from each sample was read using fluorescence at 530 nm and 590 nm excitation and emission wavelengths, respectively. Readings for a given time point were normalized to a control specific to that time point, which was 1 mg/mL alamarBlue in culture medium with no sample, also

incubated at 37°C for 3 hours. Samples were rinsed once with PBS before being returned to culture medium.

2.8 Viability imaging and histology of cell distribution through depth of samples

Chondrocyte viability was determined by staining samples with 4 µg/mL fluorescein diacetate (FDA) and 35 µg/mL propridium iodide (PI) to visualize live and dead cells, respectively. Samples were viewed using an Olympus FV 1000 confocal microscope at weekly time points to visually assess viability.

To assess the distribution of cells throughout the depth of the samples, solid scaffolds loaded with chondrocyte-seeded KLD gels (as described above) were fixed in 10% formalin at 4°C overnight after one week in culture. Samples were dehydrated in 70% ethanol, paraffin-embedded, sliced into 5 µm sections, and mounted on slides. Slides were then deparaffinized, rehydrated, and stained with 300nM DAPI to visualize cell nuclei and thus cell distribution throughout a cross-section of the samples. A Nikon Eclipse TE-300 fluorescence microscope was used to view these samples.

2.9 Statistical analysis

Values are mean ± SEM. For data with a normal distribution, one-way or two-way ANOVA was used in conjunction with post-hoc Tukey HSD. If data were not normally distributed, a Wilcoxon signed-rank test was used (JMP 12, SAS, Inc., Cary, NC).

3. Results

3.1 Cell distribution through depth of composite scaffolds

In order to visualize the ability of chondrocytes seeded in KLD hydrogels to be absorbed and evenly distributed through the depth of the solid scaffolds, histological images were taken. Samples were cultured for one week, then fixed overnight with 10% formalin and paraffin embedded before being sliced along the center (Fig 3.1A). Slices were deparafinnized and rehydrated, then stained with 300 nM DAPI to visualize cell nuclei (Fig 3.1B). In three of the solid scaffolds, P:T-2, ePTFE-1, and ePTFE-2, a bubble of hydrogel was visible on the top surface of the samples prior to fixation and processing (Fig 3.2). P:T-1 samples had a very minimal gel bubble.

Distribution of nuclei was most even in P:T-1, visible through most of the depth of the sample. P:T-1 had a thickness of 1.8 mm, and the DAPI-stained cells spread across a thickness of about 1.5 mm. P:T-2 also had a thickness of 1.8 mm, but had a larger gel bubble that increased the effective thickness of the composite scaffold. Cells were distributed along the top surface of the sample, constituting about 750 μm in depth. Some non-specific staining was visible. ePTFE-1 and ePTFE-2 showed poor cell distribution. Both materials were approximately 2.5 mm in thickness, but may have been compressed during processing. ePTFE-1 was sparsely populated with small pockets of cells that were poorly distributed, while ePTFE-2 showed a thin layer of cells on the top ~500 μm of sample.

3.2 Quantitative and qualitative analysis of cell viability over four-week culture

To quantitatively assess chondrocyte viability within composite scaffolds, an alamarBlue assay was used. At weekly time points, samples were incubated in 1 mg/mL alamarBlue in culture medium for 3 hours. Medium from each sample was transferred to a new plate and read using fluorescence at excitation and emission wavelengths of 530 nm and 590 nm, respectively. Fluorescence readings for a given time point were normalized to a control, which was 1 mg/mL in culture medium incubated for 3 hours with no sample. Readings can be directly correlated

with number of viable cells. All four materials showed statistically significant increases in the number of viable cells over the period of the long-term culture (Fig 3.3). These data showed that a population of viable chondrocytes was maintained over four-weeks in all composite scaffolds and that proliferation was occurring.

To qualitatively assess chondrocyte viability, live/dead staining was performed. Samples were stained with 4 μg/mL fluorescein diacetate (FDA) and 35 μg/mL propridium iodide (PI) to visualize live and dead cells, respectively. Samples were visualized and imaged using an Olympus FV 1000 confocal microscope. Representative images at approximately 100 μm depth from the top of the samples were taken from image stacks to demonstrate viability in that sample (Fig 3.4). FDA stained cells appear green, while PI stained cells appear red. All four materials showed maintenance of cell viability, as a dense population of green cells was visible in all images. An overall trend of proliferation was also visible in all four samples, as the density of green cells appeared to increase with culture time. Imaging less-densely packed pockets of the samples in P:T-1 and P:T-2 also allowed better visualization of individual cells and showed that some cells were able to adhere to scaffold fibers at longer time points (Fig 3.5).

3.3 Matrix production over four-week culture

To assess matrix production by chondrocytes seeded in the composite scaffolds, ^{35}S-sulfate incorporation rate and total GAG accumulation were measured. At weekly time points, samples were incubated in 5 μCi/mL of ^{35}S-sulfate in culture medium for 1-2 days. Samples were washed and digested in 0.1 mg/mL Proteinase-K. Radioactivity levels were normalized to a control of ^{35}S-sulfate culture medium from the given time point. Incorporation rate was calculated by dividing these normalized data by the hours of incubation and the DNA content of the samples (Fig 3.6). Incorporation rates in P:T-1 remained constant at about 2 nmol/hr/μg DNA for the first three weeks in culture, significantly dropping to about 0.5 nmol/hr/μg DNA at week 4. Incorporation rates in P:T-2 remained constant at about 2 nmol/hr/μg DNA for the first 2 weeks in culture, significantly dropped to about 0.1 nmol/hr/μg DNA at week 3, and significantly increased to about 6 nmol/hr/μg DNA at week 4. Rates in ePTFE-1 fluctuated between 0.7 and 10 nmol/hr/μg DNA with no statistical differences between time points. Rates in ePTFE-2

ranged from 2 and 30 nmol/hr/μg DNA, with the exception of a significant spike to about 200 nmol/hr/μg DNA at week 1. Despite the greater range in means, variance was large for these data and statistical differences were only found between week 1 and the other time points.

GAG accumulation was measured on the same Proteinase-K digested samples using DMMB dye, and was normalized by DNA content. GAG accumulation increased significantly during the four-week culture in P:T-1 and ePTFE-1, with values reaching about 300 μg GAG/μg DNA by week 4. Significant increases were also seen in ePTFE-2 samples, with levels reaching about 220 μg GAG/μg DNA by week 4. P:T-2 samples also saw a significant increase in GAG accumulation over the course of the four weeks, with values an order of magnitude higher than in other materials and reaching about 2000 μg GAG/μg DNA by week 4.

3.4 Mechanical behavior of samples under static and dynamic compression

Samples were tested under both static and dynamic compressive displacement. A 2.5% displacement ramp over 60 seconds was followed by a 240-second hold, repeated six times for a total of 15% strain. Dynamic behavior was tested using a 1% amplitude sinusoidal displacement at frequencies of 0.01, 0.02, 0.03, 0.05, 0.1, 0.2, 0.3, 0.5, and 1 Hz. P:T-1 and P:T-2 samples appeared fully hydrated in culture, so we hypothesized that gel had indeed gotten into the materials and any gel bubbles were scraped off the top of the sample prior to testing. This would hypothetically test mechanical properties of the solid-scaffold encapsulated gels without testing the properties of any free-swelling gel present on top of materials. Conversely, the side of the ePTFE materials without gel bubbles did not appear to be hydrated and caused samples to float, despite being in long-term culture, so we hypothesized that gel had not penetrated very far into the sample. If only minimal gel had penetrated the solid scaffold, it would not be possible to measure mechanical behavior of solid scaffold encapsulated gels. Rather than scrapping the samples completely, gel bubbles on ePTFE samples were left intact so that mechanical behavior of gels sitting on top of the materials could be compared to that of chondrocyte-seeded hydrogels cultured alone.

22

The equilibrium modulus of P:T-1 composite scaffold samples decreased significantly from about 100 – 130 kPa at weeks 0 and 1, respectively, to about 40 kPa at week 3 (Fig. 3.9). The modulus remained at around 40 kPa at week 4, as well, but statistical significance was not found due to higher variance at this time point. No statistically significant differences were found in the magnitude of the dynamic modulus, which ranged from about 230 – 520 kPa. Visually, values at each frequency seemed to follow a similar trend over the four weeks as the equilibrium modulus. Magnitude also appeared to increase with frequency at each time point, however again no statistical significance was found. Dynamic modulus phase significantly increased at 0.01 Hz from weeks 0 and 1 to weeks 3 and 4. A significant decrease was found from 0.01 Hz to 1 Hz in week 4 time points. No significance was found at other frequencies. Looking at the complete data (Fig. 3.8), the slope of the phase over the full frequency range appeared to shift from positive in week 0 to slightly positive at week 1 to negative in weeks 2 through 4. Phase values ranged from 6 – 18 degrees.

The equilibrium modulus of P:T-2 composite scaffold samples remained constant across the four-week culture, as no significant differences between time points was found (Fig. 3.10). Moduli ranged from 12 – 37 kPa. As with P:T-1, no statistically significant differences were found in the magnitude of the dynamic modulus, which ranged from about 230 – 520 kPa. Visually, values at each frequency seemed to follow a similar trend over the four weeks as the equilibrium modulus. Magnitude also appeared to increase with frequency at each time point, however again no statistical significance was found. Dynamic phase significantly increased over the four weeks at 0.01 Hz and 0.1 Hz, but not at 1 Hz. Grouping by time point shows significant increase in phase in weeks 0 – 2. Phase values range from about 6 – 20 degrees. The slope of the phase over the full range of frequencies (Fig. 3.8) does not appear to vary between time points, remaining positive over the duration of the culture.

The thickness of ePTFE-1 and ePTFE-2 samples with gel bubbles intact was about 4 mm, while the materials alone were about 2.5 mm (Fig. 3.11). This means that the 15% total displacement was measuring into the depth of the gel bubble and would not have reached the underlying ePTFE materials. The equilibrium modulus of ePTFE-1 composite scaffolds (i.e., the gel bubbles on top of ePTFE-1 samples) increased significantly from about 0.5 – 1 kPa at weeks 1 and 2,

respectively, to about 2.5 kPa at week 4. The dynamic modulus magnitude increased significantly from weeks 1 and 2 to weeks 3 and 4 at 0.01, 0.1 and 1 Hz. Values increased from about 5 kPa to about 25 kPa. Relative changes appeared to mirror the equilibrium modulus data. No significant differences between frequencies appeared when data were grouped by time point. Dynamic modulus phase increased significantly at 0.1 Hz, but not at other frequencies. When grouped by time point, significant decreases in phase from 0.01 Hz to 1 Hz were found at weeks 1, 2 and 4. Phase values ranged from about 10 – 20 degrees. The slope of the phase over the full range of frequencies (Fig. 3.8) did not appear to vary between time points, and was consistently negative over the duration of the culture.

The equilibrium modulus of ePTFE-2 composite scaffolds (i.e., the gel bubbles on top of the ePTFE-2 samples) appeared to increase over the four-week culture, however statistical significance was only found between weeks 2 and 3 (Fig. 3.12). Values ranged from about 0.5 – 2 kPa. The dynamic modulus magnitude significantly increased over the four weeks at 0.01, 0.1 and 1 Hz. No significant differences were found between frequencies when data were grouped by time point. Moduli ranged from about 3 – 25 kPa. Dynamic modulus phase increased significantly over the duration of the culture at 0.01 and 0.1 Hz, but not at 1 Hz. Phase decreased significantly with increasing frequency at weeks 1 – 3. Values ranged from about 5 – 20 degrees. Similar to the ePTFE-1 samples, the slope of the phase over the full range of frequencies (Fig. 3.8) did not appear to vary between time points, and was consistently negative over the duration of the culture.

3.5 Pilot study to determine integration of composite scaffolds with native tissue

A small pilot study was done to assess whether repair tissue formed in the composite scaffolds could integrate with native cartilage tissue. Cartilage explants were taken from the trochlear groove and cut into cartilage rings 1.4 mm thick (Fig 3.13A). Composite scaffolds of P:T-1 loaded with chondrocyte-seeded KLD hydrogel were cast and placed inside the cartilage rings to create complete constructs. Constructs were cultured for two weeks to analyze ^{35}S-sulfate incorporation and GAG accumulation (Fig 3.13B), as described in section 3.3. Although statistical significance could not be determined due to small sample size (n = 2), it appears that

incorporation rate remained relatively constant at around 1.5 nmol/hr/μg DNA over the two weeks. GAG accumulation appeared to increase over the two weeks, reaching about 200 μg GAG/μg DNA at week 2. Integration of repair tissue in the composite scaffold with native cartilage tissue was determined by tracking cell migration from the composite scaffold into the cartilage ring. Chondrocytes were stained with CFSE before seeding in KLD hydrogels. Samples were visualized and imaged with confocal microscopy (Fig 3.13). Week 1 imaging showed that the cells had not been distributed evenly to the edge of the composite scaffold, and were not present at the interface between the composite scaffold and the cartilage ring. The sample imaged at week 2 appeared to have slightly better initial cell distribution, and a few individual cells appeared to have migrated across the interface into the cartilage ring.
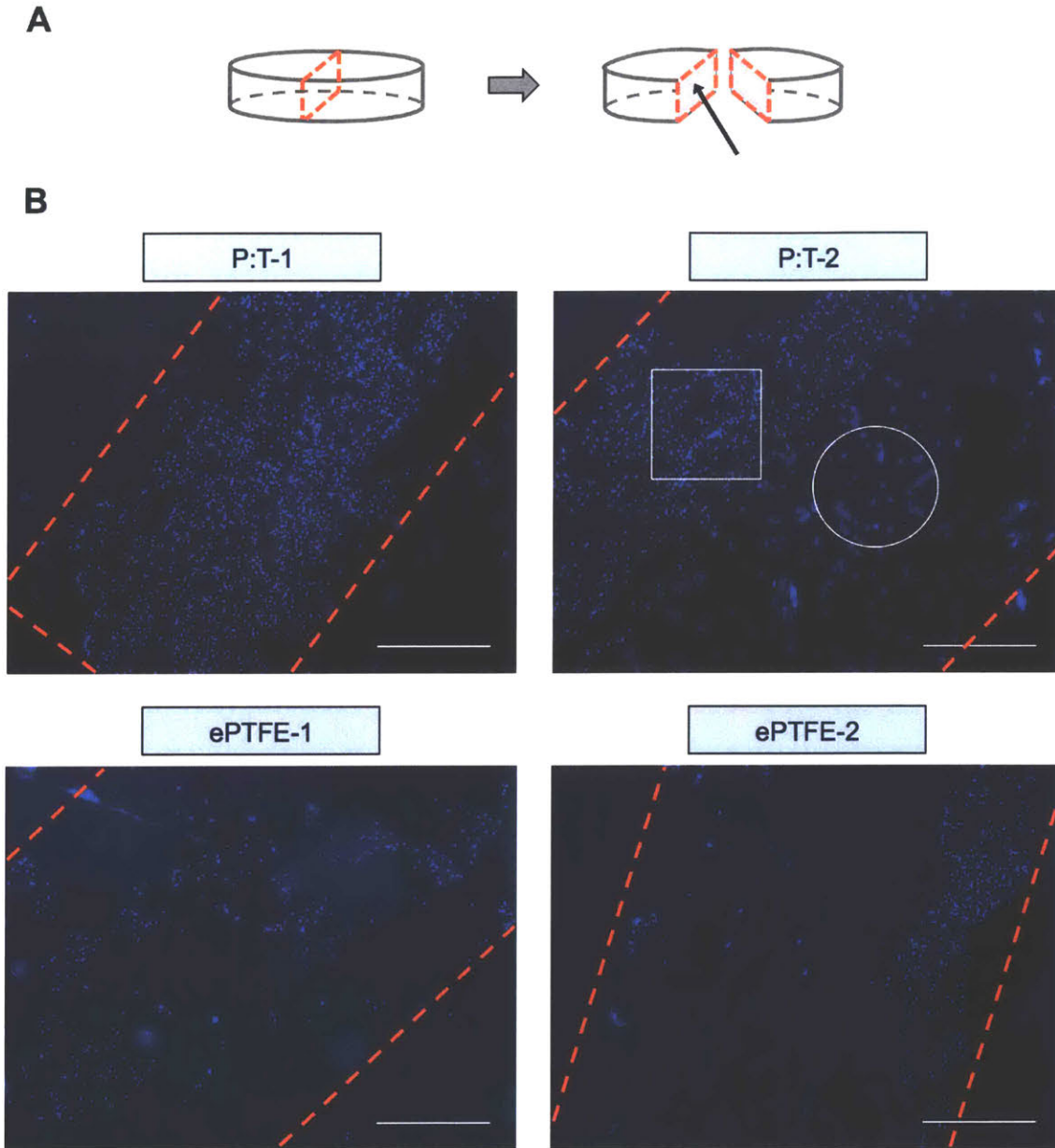
A

B

Figure 3.1: Visualization of cell distribution through depth of composite scaffold constructs. (A) Schematic showing the origin of the slices used for staining. Paraffin-embedded fixed samples were sliced along the diameter (indicated by red dotted rectangle). A 5 µm slice was taken from the inner surface of the sample (indicated by the black arrow). (B) Histological images showing cell distribution. Slices were stained with 300 nM DAPI to visualize chondrocyte nuclei. Approximate perimeter of the samples (the red dotted rectangle from part A) is marked in red dotted lines. Distinction between cell nuclei staining (white rectangle) and non-specific staining (white circle) is shown. Scale bars = 500 µm.
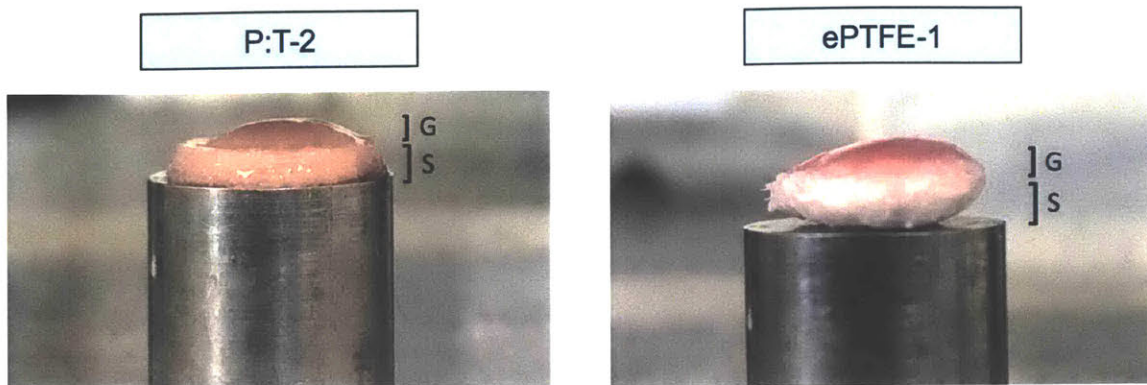
Figure 3.2: Examples of gel bubbles present on top of samples. Composite scaffolds and gel bubbles are indicated by S and G, respectively.
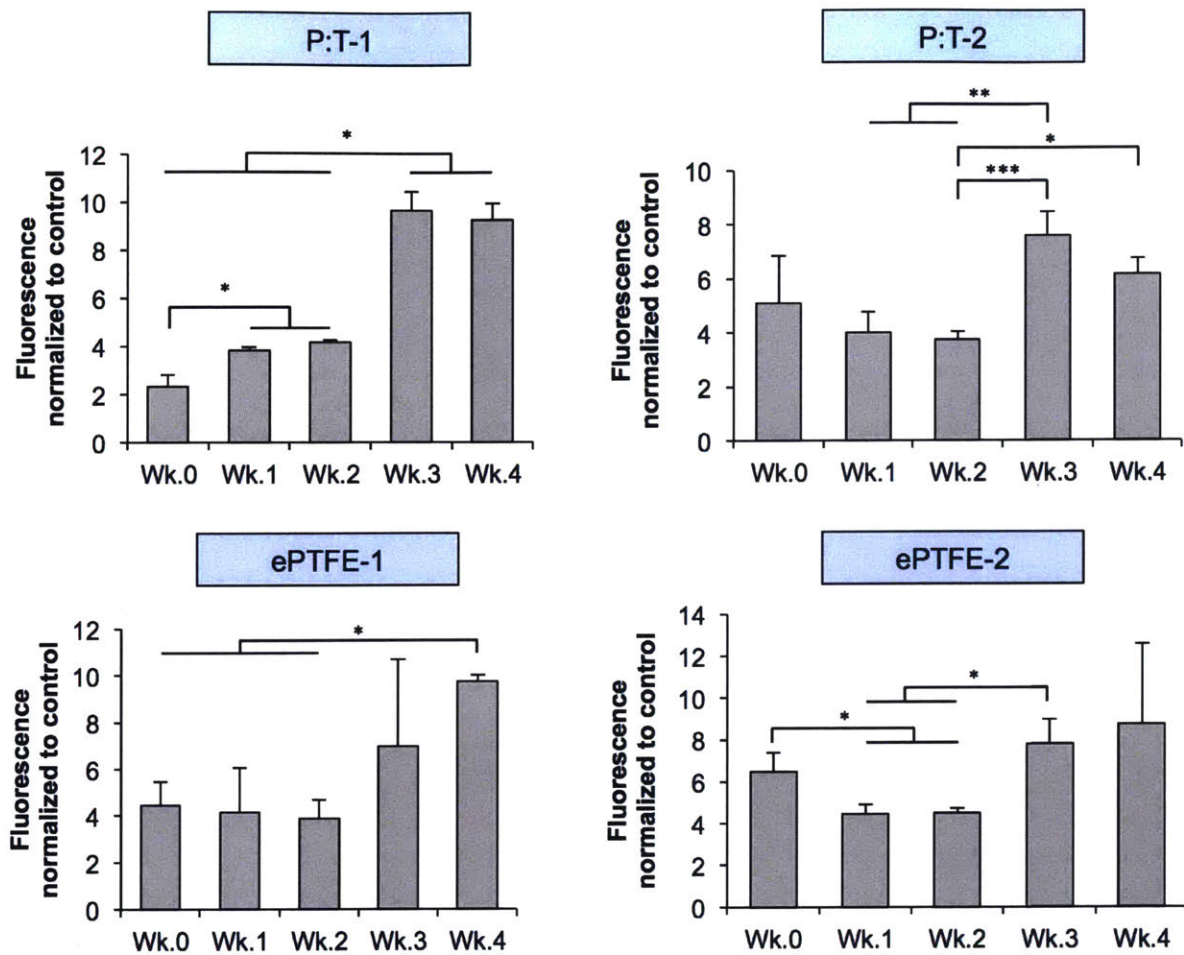
Figure 3.3: Quantitative chondrocyte viability over four-week culture. Samples were incubated in 1 mg/mL alamarBlue in culture medium for 3 hours. A control of 1 mg/mL alamarBlue in culture medium with no sample was also incubated. Medium from each sample and control was read using an excitation wavelength of 530 nm and an emission wavelength of 590 nm. Sample fluorescence was normalized to control. (n = 4, * $p < 0.05$, ** $p < 0.01$, *** $p < 0.001$)

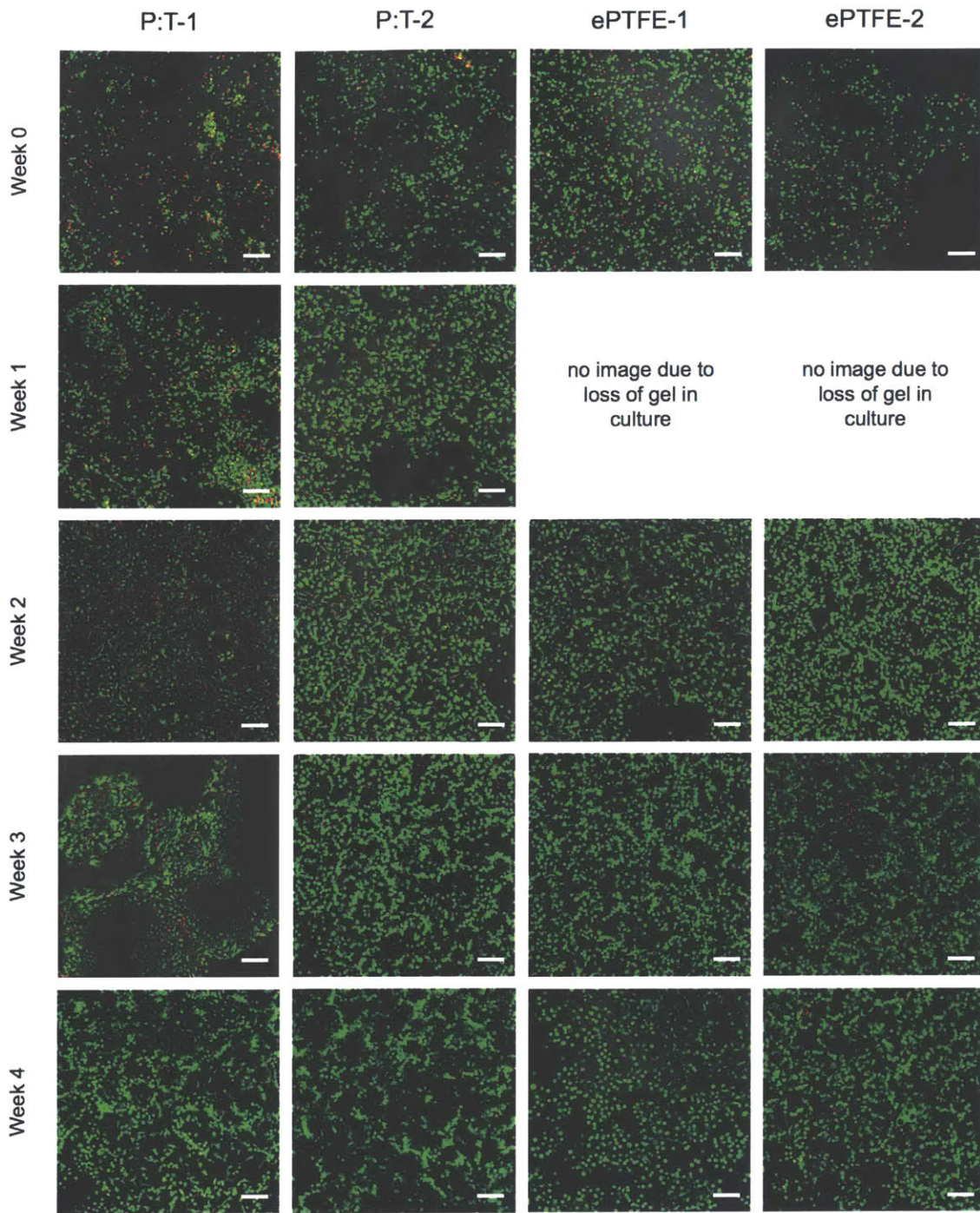|	P:T-1	P:T-2	ePTFE-1	ePTFE-2
Week 0				
Week 1			no image due to loss of gel in culture	no image due to loss of gel in culture
Week 2				
Week 3				
Week 4				

Figure 3.4: Qualitative chondrocyte viability over four-week culture. Each week, one sample was sacrificed to qualitatively assess cell viability. Samples were stained with 4 μg/mL fluorescein diacetate (FDA) and 35 μg/mL propridium iodide (PI) to visualize live and dead cells, respectively. Samples were viewed using an Olympus FV 1000 confocal microscope. Gels in ePTFE-1 and ePTFE-2 samples at week 1 were damaged during transfer between plates, so images are unavailable. Scale bars = 100 μm.

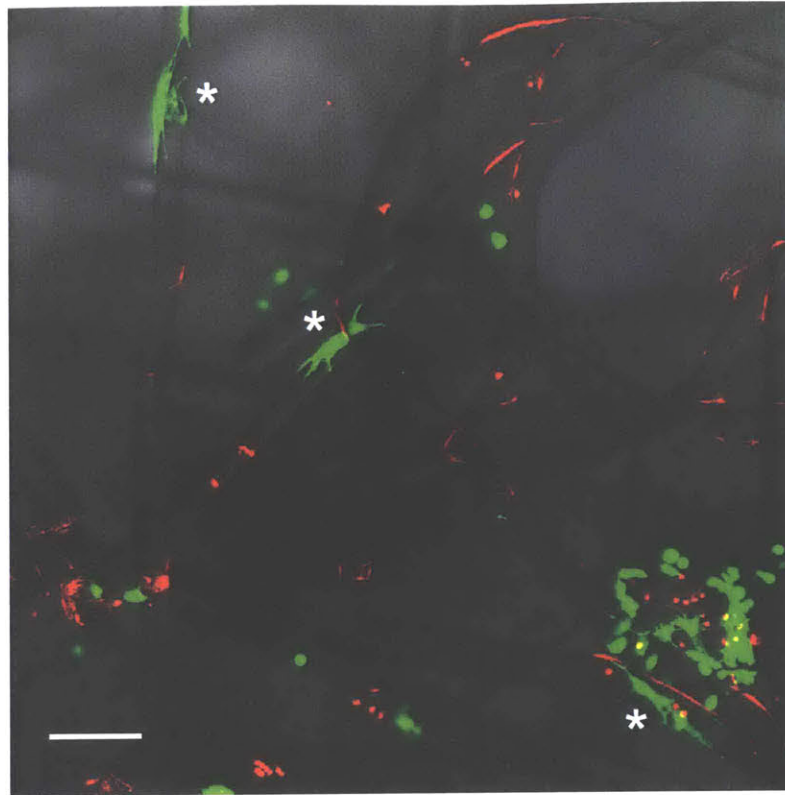**Figure 3.5**: Chondrocyte adhesion to P:T-1 scaffold fibers. This sample was stained after three weeks in culture with 4 μg/mL fluorescein diacetate (FDA) and 35 μg/mL propridium iodide (PI) to visualize live and dead cells, respectively. Samples were viewed using an Olympus FV 1000 confocal microscope. Cells of interest showing adhesion to fibers are marked with *. Scale bar = 100 μm.
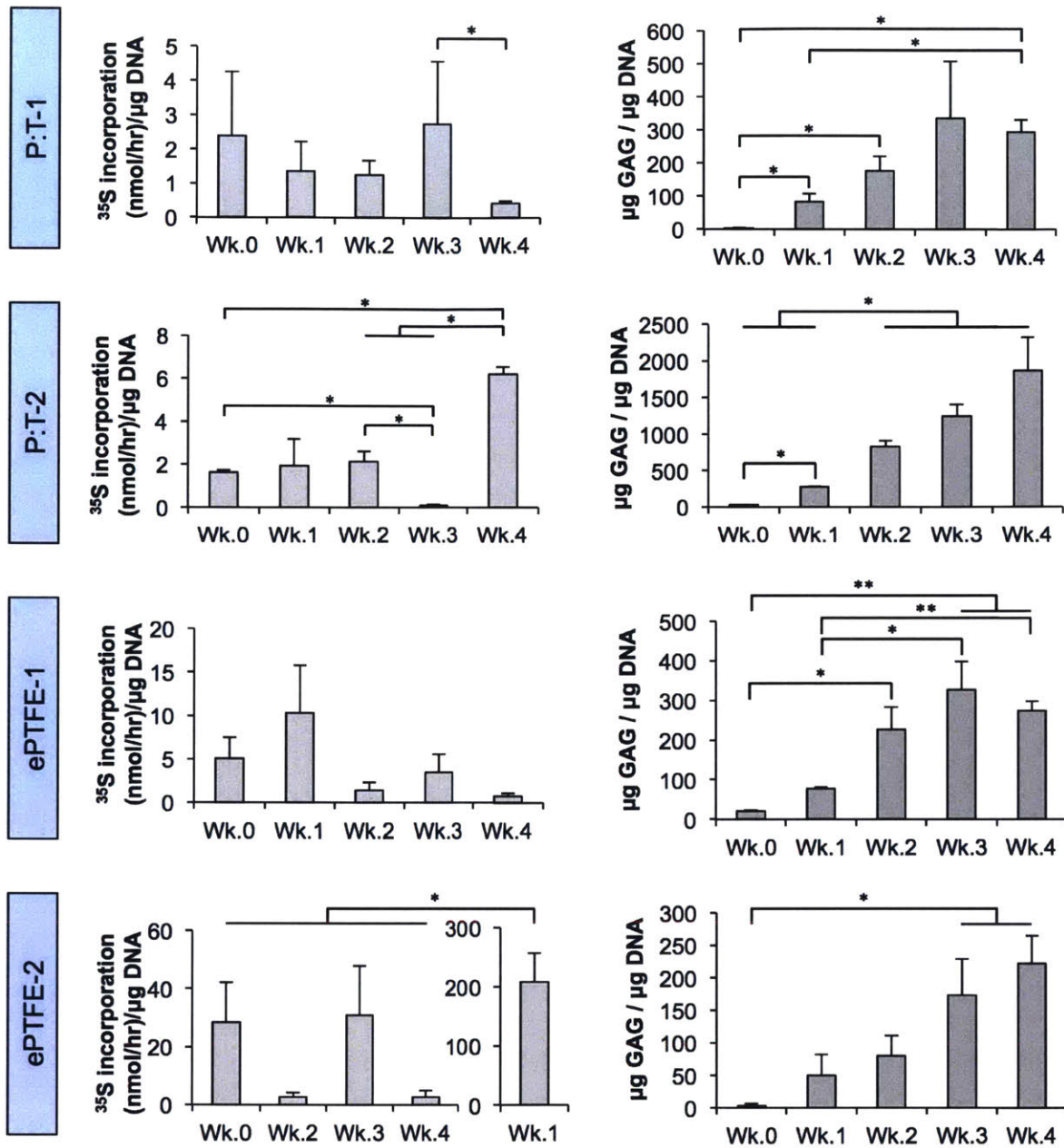
Figure 3.6: Sulfate incorporation and GAG accumulation over four-week culture. Sulfate incorporation was measured by supplementing culture medium with 5 μCi/mL of ^{35}S-sulfate and incubating for 1 – 2 days. Samples were digested with 0.1 mg/mL Proteinase-K. These digests were then used to measure DNA and GAG content using PicoGreen and DMMB dye, respectively. (n = 4, * p < 0.05, ** p < 0.01, *** p < 0.001)

Figure 3.7: Dynamic modulus magnitude during four-week culture. Composite scaffold samples were tested in unconfined compression with 1% amplitude sinusoidal strain at frequencies of 0.01, 0.02, 0.03, 0.05, 0.1, 0.2, 0.3, 0.5, and 1 Hz. Legend in P:T-2 applies to all plots. (n = 4)

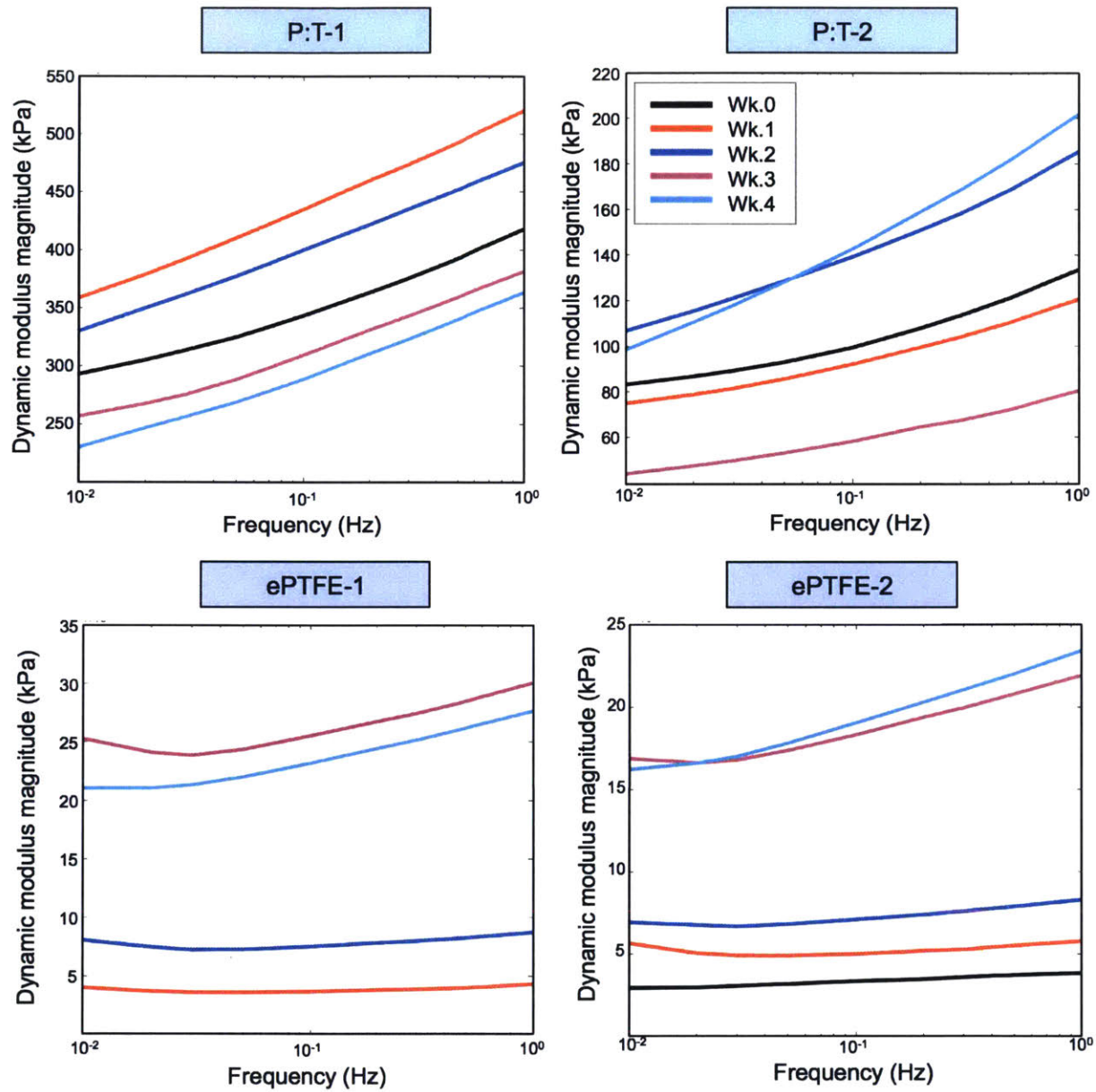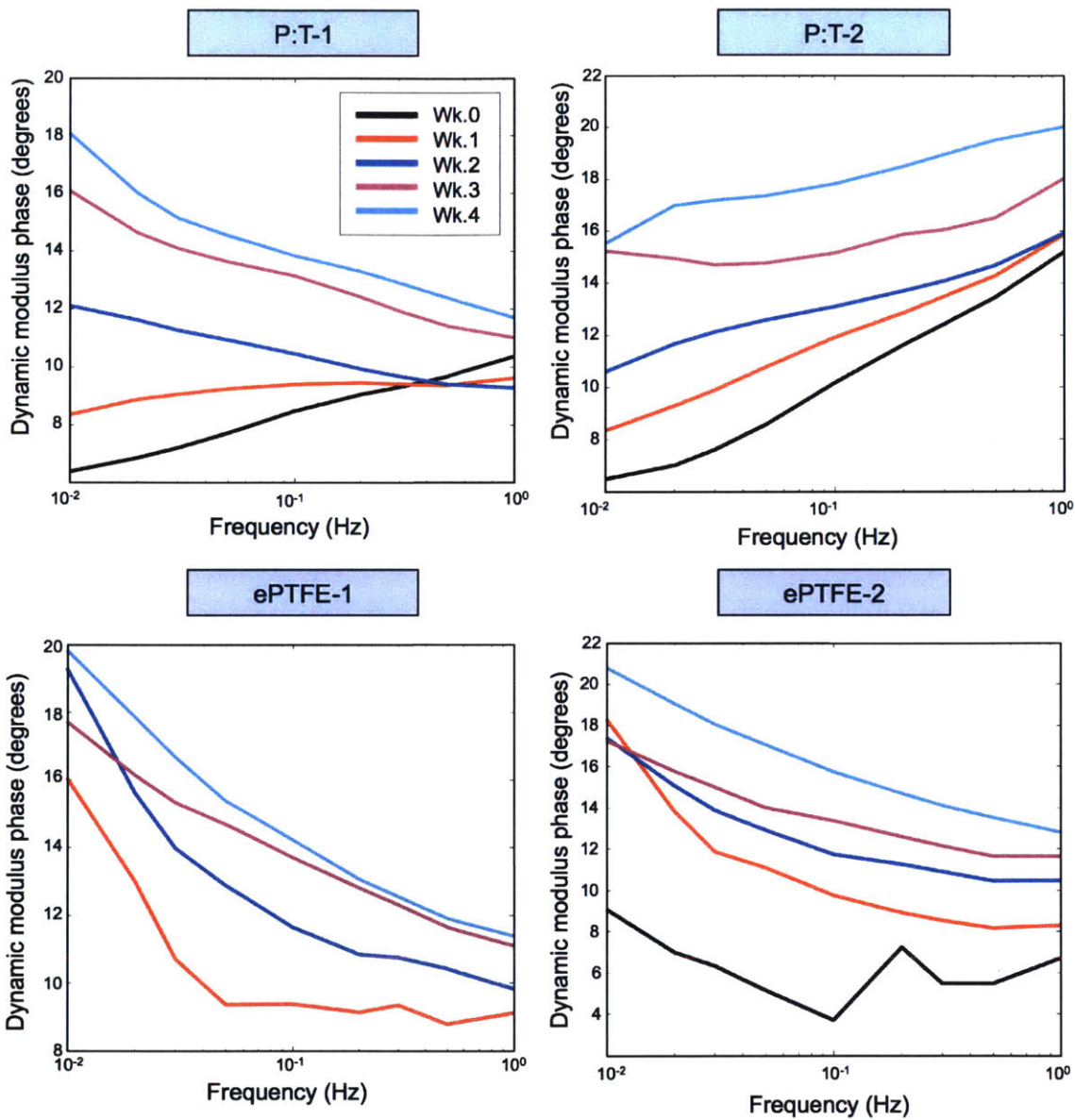**Figure 3.8**: Dynamic modulus phase during four-week culture. Composite scaffold samples were tested in unconfined compression with 1% amplitude sinusoidal strain at frequencies of 0.01, 0.02, 0.03, 0.05, 0.1, 0.2, 0.3, 0.5, and 1 Hz. Legend in P:T-1 applies to all plots. (n = 4)

Figure 3.9: Mechanical behavior of P:T-1 over four-week culture. (A) Equilibrium behavior of composite scaffolds. P:T-1 samples loaded with chondrocyte-seeded KLD hydrogels were tested under unconfined compression, with 2.5% ramp and hold repeated 6 times for 15% total strain. (n = 4, * p < 0.05) (B) Dynamic modulus magnitude and phase behavior of composite scaffolds. Samples were tested in unconfined compression with 1% amplitude sinusoidal strain at frequencies from 0.01 – 1 Hz. Dynamic modulus magnitude and phase are shown clustered by both frequency and time point. (n = 4, * p < 0.05, *** p < 0.001)

Figure 3.10: Mechanical behavior of P:T-2 over four-week culture. (A) Equilibrium behavior of composite scaffolds. P:T-2 samples loaded with chondrocyte-seeded KLD hydrogels were tested under unconfined compression, with 2.5% ramp and hold repeated 6 times for 15% total strain. (n = 4) (B) Dynamic modulus magnitude and phase behavior of composite scaffolds. Samples were tested in unconfined compression with 1% amplitude sinusoidal strain at frequencies from 0.01 – 1 Hz. Dynamic modulus magnitude and phase are shown clustered by both frequency and time point. (n = 4, * $p < 0.05$, ** $p < 0.01$, *** $p < 0.001$)
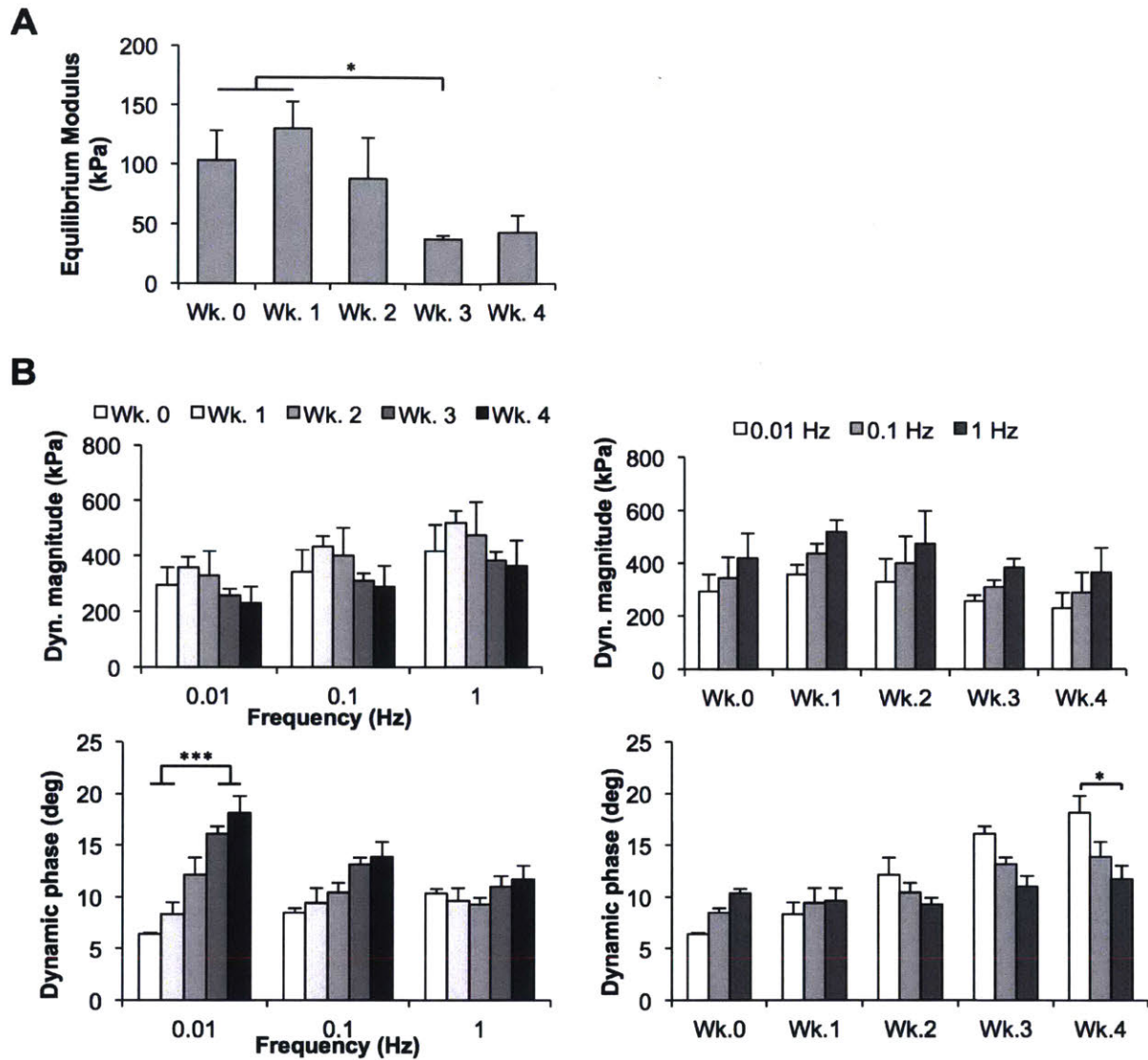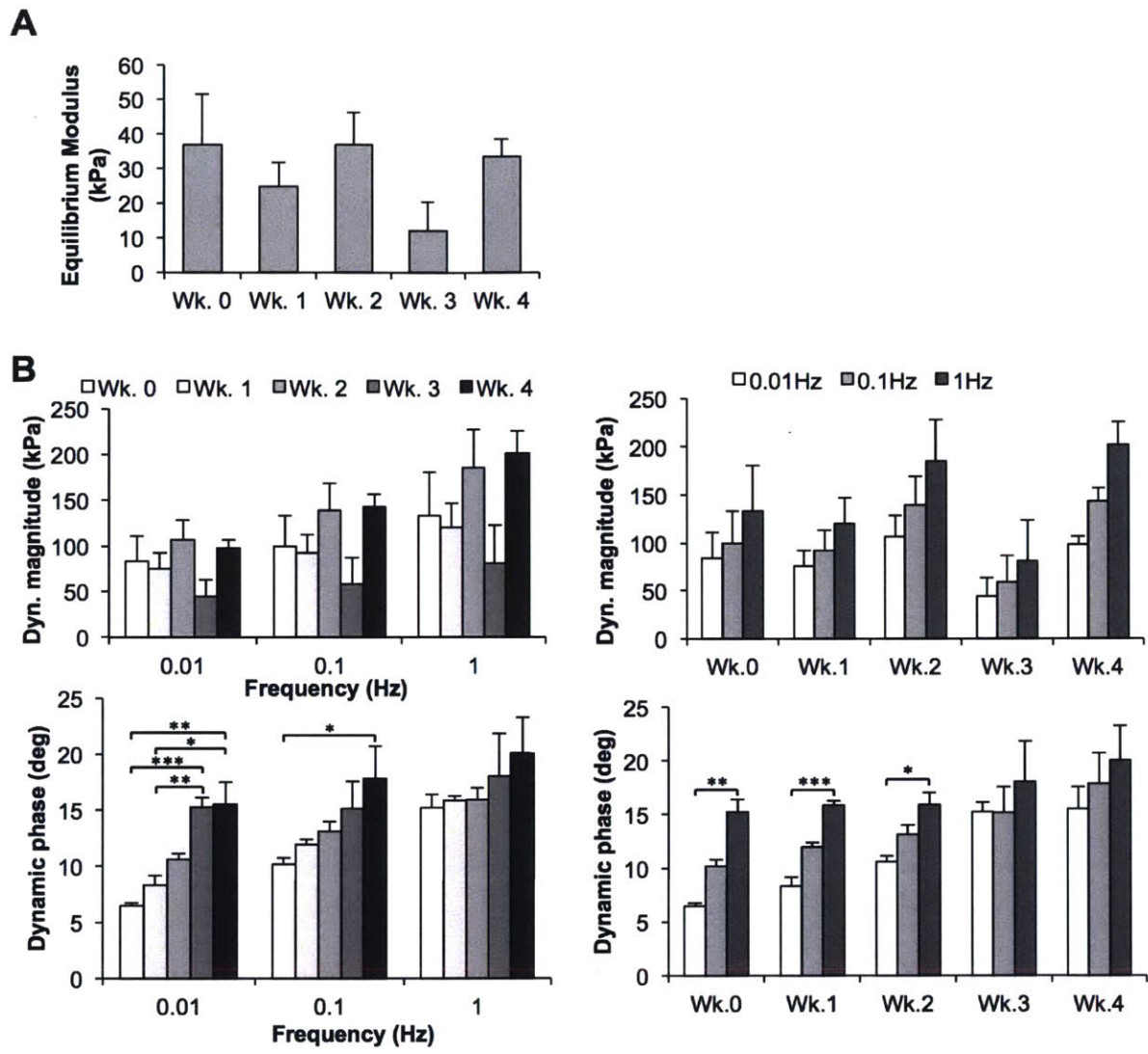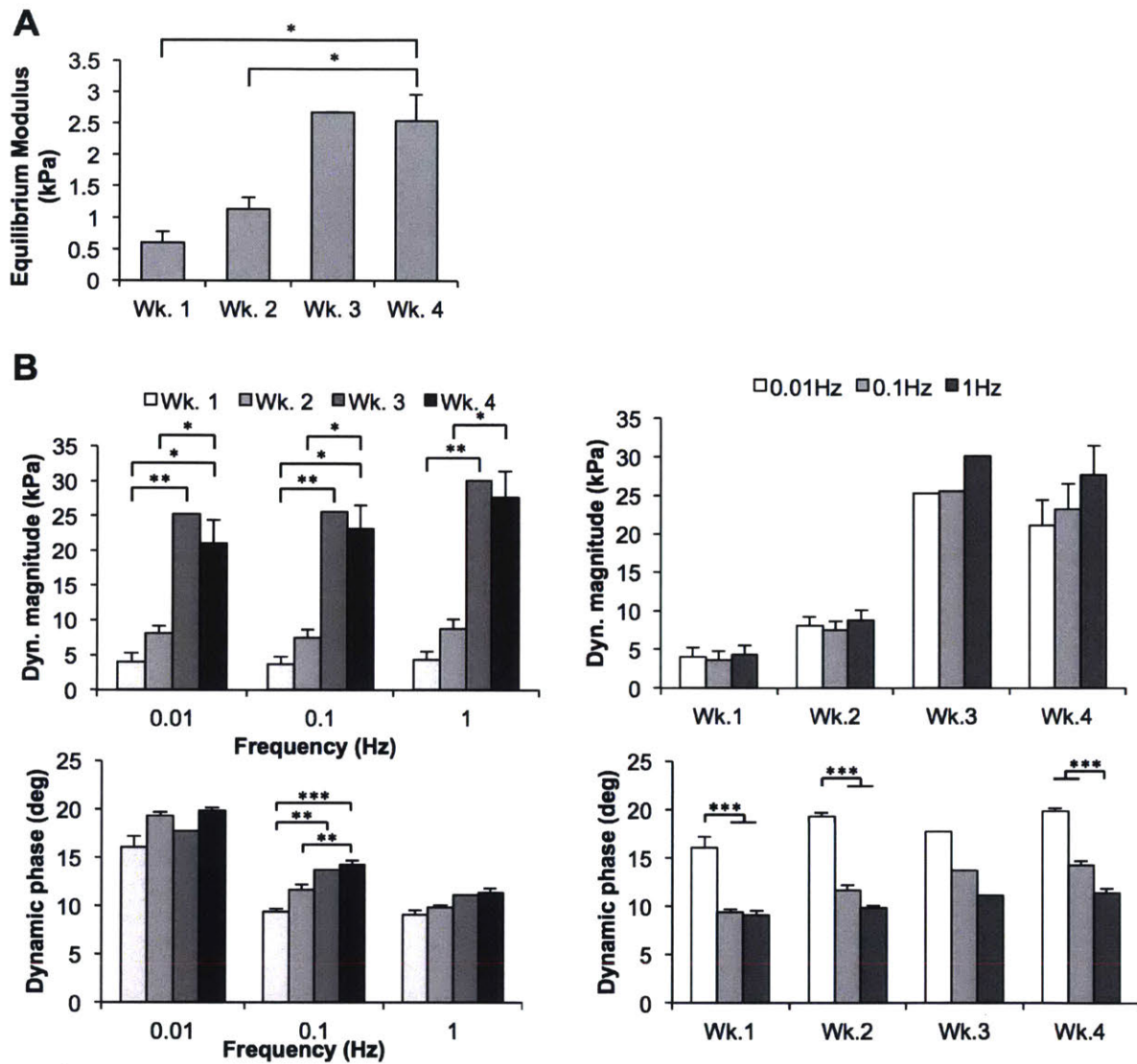
Figure 3.11: Mechanical behavior of ePTFE-1 over four-week culture. (A) Equilibrium behavior of composite scaffolds. ePTFE-1 samples loaded with chondrocyte-seeded KLD hydrogels were tested under unconfined compression, with 2.5% ramp and hold repeated 6 times for 15% total strain. Week 0 samples were lost in culture and data were unavailable. (n = 4, except for week 3 which was n = 1, * $p < 0.05$) (B) Dynamic modulus magnitude and phase behavior of composite scaffolds. Samples were tested in unconfined compression with 1% amplitude sinusoidal strain at frequencies from 0.01 – 1 Hz. Dynamic modulus magnitude and phase are shown clustered by both frequency and time point. Week 0 samples were lost in culture and data were unavailable. (n = 4, except for week 3 which was n = 1, * $p < 0.05$, ** $p < 0.01$ *** $p < 0.001$)
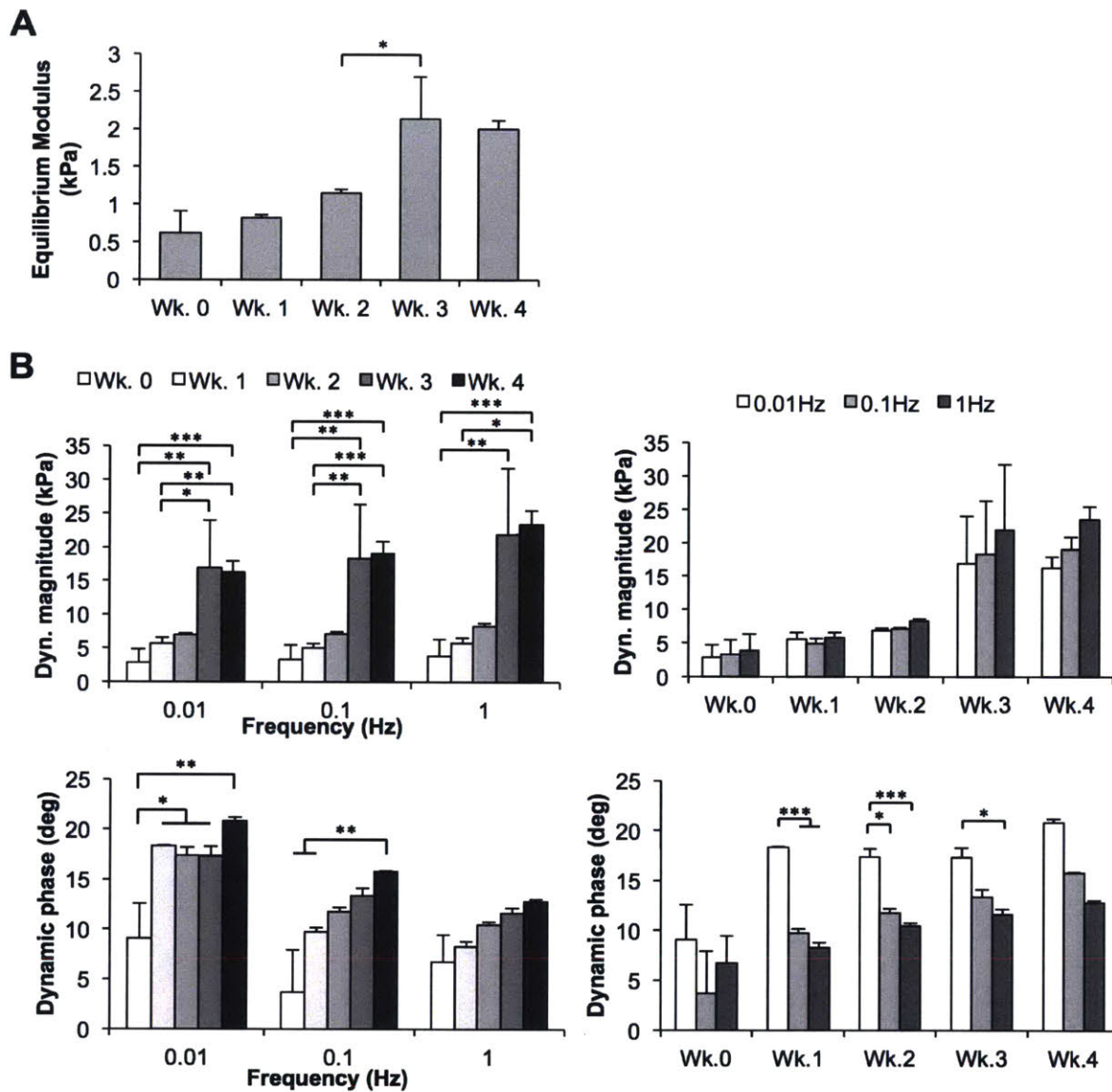
Figure 3.12: Mechanical behavior of ePTFE-2 over four-week culture. (A) Equilibrium behavior of composite scaffolds. ePTFE-2 samples loaded with chondrocyte-seeded KLD hydrogels were tested under unconfined compression, with 2.5% ramp and hold repeated 6 times for 15% total strain. (n = 4, * p < 0.05) (B) Dynamic modulus magnitude and phase behavior of composite scaffolds. Samples were tested in unconfined compression with 1% amplitude sinusoidal strain at frequencies from 0.01 – 1 Hz. Dynamic modulus magnitude and phase are shown clustered by both frequency and time point. (n = 4, * p < 0.05, ** p < 0.01, *** p < 0.001)
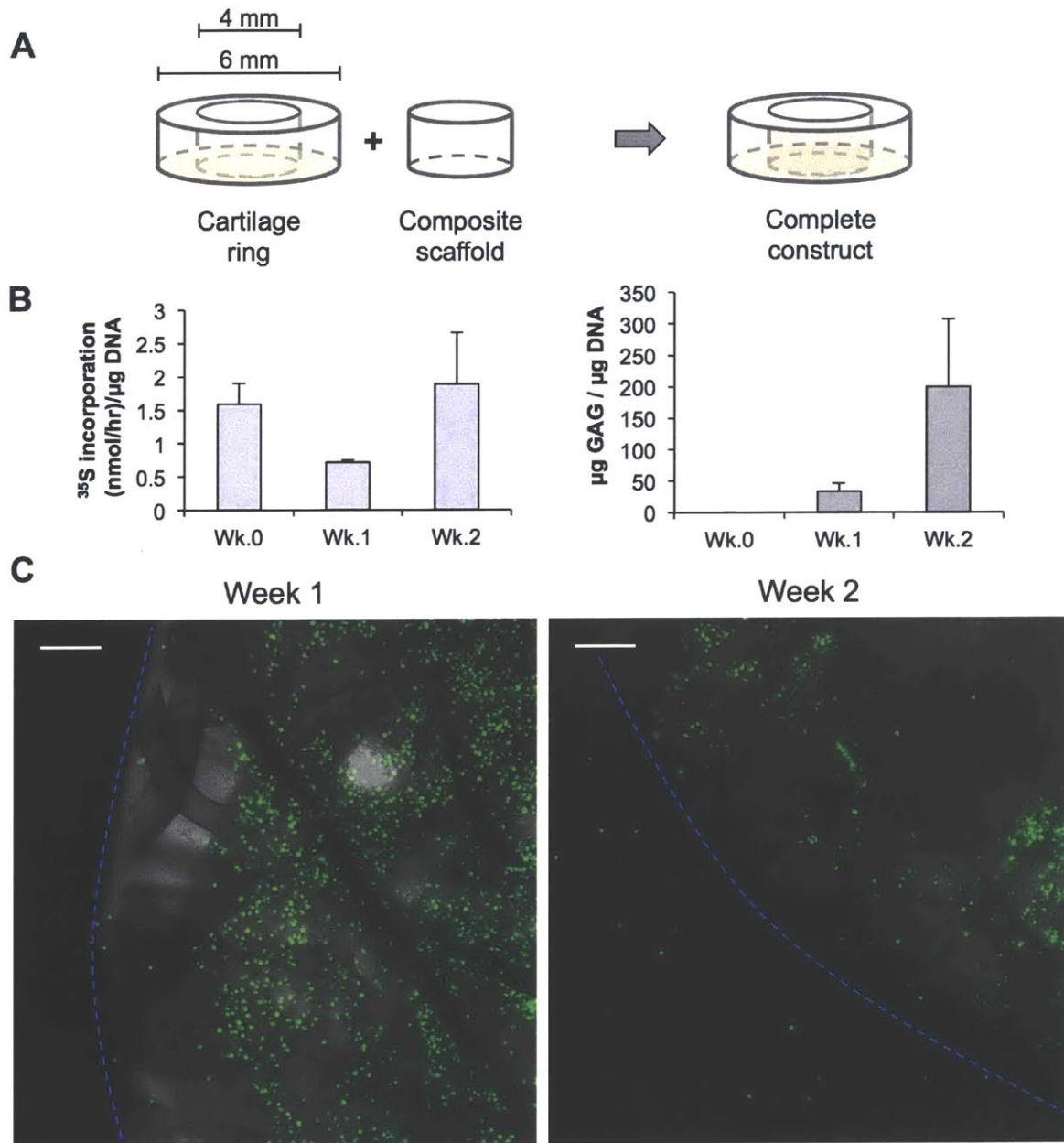
Figure 3.13: Pilot study of composite scaffold integration with native tissue in cartilage defect model. (A) Schematic of defect model. Composite scaffolds of P:T-1 loaded with chondrocyte-seeded KLD hydrogel were placed in the center of trypsin-pretreated cartilage rings to create the complete construct. (B) Matrix production of chondrocytes in composite scaffold. 5 µCi/mL ^{35}S-sulfate was added to media at weekly time points. Constructs were washed and cartilage rings were removed before digesting the remaining composite scaffold in 0.1 mg/mL Proteinase-K. DNA and GAG content were measured by PicoGreen and DMMB, respectively. (n = 2) (C) Visualization of integration between repair scaffold and native tissue. Chondrocytes were dyed with CFSE before seeding in KLD hydrogel. The interface between the scaffold and native cartilage is shown (blue dotted line). Scale bars = 100 µm.

4. Discussion

Tissue engineering approaches to the repair of articular cartilage defects in PTOA have made use of a variety of synthetic and naturally derived materials. Cell-seeded hydrogels have shown pro-chondrogenic effects and encourage matrix production and proliferation.[38, 40] However, these gels are often very soft at early time points before cells have produced enough matrix to provide mechanical strength.[39] An alternative approach has been solid scaffolds, which are mechanically robust at early time points but have inferior bioactivity and integration compared to their hydrogel counterparts.[41] Composite scaffolds are an emerging strategy to combat the problems of hydrogels and solid scaffolds by combining the two. The solid scaffold provides the mechanical protection at early time points while the hydrogel provides a favorable environment for cells to create cartilage-like repair tissue. This has been the motivation for this work, in which synthetic solid bioabsorbable PGA:TMC or ePTFE scaffolds were loaded with chondrocyte-seeded self-assembling KLD hydrogels to create composite scaffolds for use in cartilage defect repair.

We confirmed that chondrocytes are able to proliferate and remain viable in the composite scaffolds for all materials tested (Fig 3.3, 3.4). This was especially promising in the P:T-1 samples, as the histological images (Fig 3.1) showed that this material had the most even cell distribution. It has been shown that cells maintain viability in the KLD hydrogels alone, with a near-two-fold increase in cell density over two weeks in culture.[50] Data from work here show that the presence of the synthetic scaffolds, either encapsulating the gels in the case of P:T-1 or acting as a platform underneath bubbles of gel in the case of the other materials, does not have a negative effect on viability or proliferation of chondrocytes. The amount of viable cells in P:T-1 samples increased approximately two-fold over the first two weeks in culture, and nearly five-fold by the end of four weeks in culture (Fig 3.3). While chondrocyte proliferation is low in adult native articular cartilage, higher proliferation may be necessary in scaffolds used for defect repair. In the native tissue, cells are already surrounded by dense extracellular matrix and can have low proliferative and anabolic activity without sacrificing integrity of the tissue as a whole. In early stages of tissue engineered scaffolds, like the composite scaffolds used here, cells will sense the lack of dense ECM that they prefer and will begin to remedy that by producing matrix.

Proliferation of cells would aid in this effort, as a greater cell population can produce the necessary ECM more quickly. Results here show that cells in our composite scaffolds have proliferative activity in addition to per-cell matrix production, which would allow for an increasing rate of overall per-construct matrix accumulation.

As mentioned above, the ^{35}S-sulfate incorporation and GAG accumulation data show that there is high per-cell matrix production in these composite scaffolds (Fig 3.6). Incorporation rates are about an order of magnitude higher than in KLD hydrogels alone, indicating that there is higher matrix production when the hydrogels are incorporated into the solid scaffold materials (Fig 4.1A). The high incorporation rates even at week 0 suggest that the cells are able to sense the lack of ECM proteins, and begin synthesizing new matrix to remedy this as soon as they enter the composite scaffold environment. This also indicates that the composite scaffold environments are not too densely packed. If scaffolds were too densely packed, the cells would sense a dense surrounding environment, and may be misled into not producing the ECM proteins necessary to create physiologically accurate repair tissue. The high incorporation rates indicate that this is not an issue in our samples, and the cells begin creating cartilage-like matrix to eventually form repair tissue that closely mimics native articular cartilage. This is especially important in the bioabsorbable PGA:TMC scaffolds, which will eventually degrade and leave behind only the cells and any matrix they have produced. It is important that enough matrix is produced to create mechanically robust neotissue before the solid scaffold degrades completely and its mechanical protection is gone. Ideally, the degradation rate of a solid scaffold should be matched in order to provide mechanical support to the hydrogel-encapsulated cells and neotissue for as long or short as necessary.

The increasing GAG accumulation seen here in all composite scaffolds indicates that newly produced matrix proteins, which we know are being made based on the ^{35}S-sulfate incorporation, are retained in the repair tissue. Had newly synthesized matrix proteins been diffusing out of the scaffolds, we would not see the accumulation of GAG over the course of the four-week culture. For P:T-1 and both ePTFE materials, GAG accumulation per cell is about half to a full order of magnitude higher than in KLD hydrogels alone (Fig 4.1A). This is consistent with incorporation rates being about an order of magnitude higher than in the gels alone. It is unclear why the GAG

accumulation in P:T-2 was an order of magnitude higher than in the other three materials, especially given that incorporation rates were comparable. There could have been inconsistency in the amount of gel extracted from the samples during the Proteinase-K digestion step, however it seems that this would have led to skewed results in the incorporation rates, as well. It may be necessary to repeat these experiments in order to confirm the validity of this result.

The presence of gel bubbles (Fig 3.2) made it difficult to measure the mechanical behavior of composite scaffolds for the ePTFE materials. As seen in the image, the region of the scaffold that did not have the gel bubble remained white through the duration of the culture, in contrast to the PGA:TMC materials which were pink from the absorbance of medium. This suggested that there was minimal absorption of the cell-seeded gel into the solid scaffold. Had the gel bubble been scraped off, it is likely that there would be very little gel remaining in the sample and the mechanical testing would only reveal the behavior of the ePTFE materials alone. In order to gain information from the experiment, albeit not the information we had originally intended to gain, we left the gel bubbles intact to determine if the mechanical behavior of the gel changed when it was on top of the ePTFE samples versus in culture alone (Fig 4.1). These results will be discussed below. While wettability was tested at the beginning of this work to determine which materials to move forward with, there may have been batch-to-batch variance as a new batch of the materials was used for the long-term culture studies. The properties of these materials may need to be adjusted to increase hydrophilicity in order to make them viable candidates for a composite scaffold approach to cartilage repair. The methods of casting the gels inside the solid scaffolds may also need to be revisited in order to ensure more even penetration and distribution throughout the scaffolds. This is true for P:T-2, as well, which we saw from the DAPI-stained histology was not able to evenly absorb the cell-seeded hydrogel as well as was initially thought.

Although the matrix production and accumulation per cell (i.e., per μg DNA) is higher in the gel bubbles on top of the ePTFE samples than in the gel-only studies, the stiffness does not reach the levels of the gel controls over a four-week culture (Fig 3.6, 3.11, 3.12, 4.1). To explain this discrepancy, we estimated the total GAG accumulation in the entire composite scaffold sample. The amount of gel present in these samples was about 50 μL, which is about 50 mg of wet weight given the high water content of KLD, while the total amount of GAG present at week 4

41

was about 50-100 µg. This means the GAG content per wet weight at week 4 was on the order of 1 µg GAG/ mg wet weight. In the gel-only controls, the GAG content per wet weight reached about 5 µg GAG/mg wet weight at day 16 and about 12 µg GAG/mg wet weight by day 39 (Fig 4.1B). This indicates that although the matrix production per cell in the composite scaffolds was very high, the total amount of GAG was low and was insufficient to increase the stiffness of the gel bubbles to the levels seen in the KLD-only controls. This problem could be addressed by increasing the cell-seeding density for future experiments to ensure that both per-cell and overall matrix production is high.

The motivation for this work was to mechanically support soft hydrogels with solid scaffolds at early time points in order to allow cells inside those hydrogels to create repair tissue without risk of damage from joint articulation. Results from the P:T-1 samples indicate that the mechanical behavior of the composite scaffolds is dominated by the mechanics of the solid scaffold at early time points (Fig 3.9). The equilibrium modulus values of the composite scaffold samples are much higher than previously measured in KLD gels alone (Fig. 4.1), which suggests that the stiffness of the scaffold is indeed dominating over the course of the four-week culture. The decrease in modulus suggests degradation of the P:T-1 over this time scale. However, at week 4 the equilibrium modulus was still about 50 kPa, indicating that the solid scaffold was at least partially intact at the end of the culture. The stiffness of the chondrocyte-seeded hydrogels on top of the ePTFE materials only reached about 2 kPa by week 4, so it is likely that the gel encapsulated in the P:T-1 scaffolds would have shown similar stiffness had it been isolated from the composite scaffold. For this reason, it appears that the week 4 mechanical behavior is still dominated by the stiffness of the P:T-1 remaining, and we are not yet able to see the mechanics of the neotissue forming in the gel portions of the composite scaffold. Again, this may be due to the fact that while GAG accumulation per cell is high, total GAG content of the construct was not high enough by 4 weeks for gel stiffness to become dominant. This could be improved by increasing cell density upon initial seeding. For the P:T-2 samples, the equilibrium stiffness again is much higher than we would expect for the gel alone, indicating that solid scaffold stiffness dominates. Conversely, the equilibrium stiffnesses of the ePTFE composite scaffolds are on the order of the starting stiffnesses of the KLD-only controls (Fig. 4.1), supporting the

42

hypothesis that we were measuring the properties of the gel bubbles on top rather than a true composite scaffold of gel-loaded ePTFE.

Previously, dynamic behavior data measured in native cartilage disks was fit to a poroelastic model, which was able to accurately predict both magnitude and phase of the data (Fig 4.2). We hypothesize that the composite scaffolds in our study are also exhibiting poroelasticity, especially over long culture periods where chondrocytes are creating cartilage-like matrix. Although no statistical significance was found in the dynamic modulus magnitudes of the PGA:TMC composite scaffolds, we can visually see a self-stiffening trend in which the magnitude increases with frequency. This behavior appears to be consistent across time points, as the solid scaffold mechanics are still dominating during the four-week culture. In the ePTFE samples, though, the self-stiffening behavior appears to increase over the course of the four weeks. The slope of the dynamic modulus magnitude over the full range of frequencies tested appears to increase with time in these materials (Fig 3.7). Previously, it has been found that self-stiffening behavior increases with depth from the surface of native articular cartilage due to the increase in GAG content.[54, 55] The increase in self-stiffening behavior of the gel bubbles in the ePTFE samples suggests that the GAG content of the gels is increasing, as well.

Assuming poroelasticity in our samples, the phase response can be fitted to the poroelastic model to determine the peak frequency of the phase (Fig 4.2). At the small range of frequencies tested in this study, a positive slope would indicate that the peak frequency is at a greater frequency than the range tested, while a negative slope would indicate that the peak frequency is at a smaller frequency than the range tested. Shifts in the slopes of the phase can thus be interpreted as shifts in the peak frequency, which is characteristic of poroelastic behavior. The peak frequency is proportional to the product of the equilibrium modulus, E, and the hydraulic permeability, k. In the P:T-1 samples, we see a shift in the slope of the phase from positive to negative, which suggests a downward shift in the peak frequency. This is consistent with the downward shift we see in the equilibrium modulus, and could also indicate a decrease in hydraulic permeability as GAG is being produced. If we were to continue the culture for longer time periods, we might expect to see further shifts of this peak, as the cells produce more ECM and further decrease hydraulic permeability. This shift may be slowed by increases in

43

equilibrium modulus as the neotissue becomes stiffer, but it is difficult to predict exactly whether increases in E or decreases in k would dominate. The other three materials do not appear to show a shift in peak frequency of the phase. In the ePTFE materials in which the gel bubble mechanics were being tested, it is likely that not enough total GAG had been produced to greatly affect hydraulic permeability, and changes in equilibrium modulus were fairly small. Since both E and k were minimally affected, we would not expect the peak frequency to shift. In the P:T-2 samples, it is possible that removal of the gel bubbles prior to mechanical testing may have removed a large proportion of the gel present in the sample, as histology showed poor cell distribution through the depth of the material (Fig 3.1). If this were the case, even though GAG accumulation was quite high (Fig 3.6), most of the newly synthesized matrix may have been scraped off. This would make any changes in hydraulic permeability unlikely. In combination with the lack of significant changes in equilibrium modulus, this explains why we do not see a shift in the peak frequency of the phase for the P:T-2 composite scaffolds.

Many existing approaches to articular cartilage repair struggle with integration of repair tissue with the native cartilage.[57] To predict whether integration would be successful with the composite scaffolds in this study, a small pilot study was performed in which the P:T-1 composite scaffolds were placed within cartilage explant rings for a two week culture (Fig 3.13A). P:T-1 was chosen over the other materials due to its superior cell distribution (Fig 3.1), lack of significant gel bubbles, and promising dynamic mechanical behavior, as discussed above. To ensure that the presence of the native tissue would not negatively affect the matrix production seen in the composite scaffolds alone, ^{35}S-sulfate incorporation and GAG accumulation studies were repeated. Values for incorporation rate and GAG accumulation were similar to those found at the two-week time point in the composite scaffolds alone (Fig 3.6, 3.13B). This confirmed that per-cell matrix production was still high in the presence of native cartilage. At week 1, chondrocytes in the composite scaffold, which had been dyed with CFSE prior to seeding in the KLD, were imaged with confocal microscopy to determine if any migration across the scaffold-native tissue interface had occurred (Fig 3.13C). This image revealed that the cells had not been distributed all the way to the edge of the composite scaffold during seeding. There was a 100 − 200 μm gap between the edge of the cells and the interface. This is problematic because cells would have to first migrate this distance to the interface and then continue to migrate even

44

further into the native tissue in order for integration to occur. This would certainly delay any migration into the native tissue and could prevent integration of the repair construct at early time points. This result revealed the necessity for better methods to ensure even cell-seeded gel distribution through the entire volume of the composite scaffolds during the casting process. The image at week 2, which was of a different sample, suggests that this gap between the cells and the edge of the composite scaffold may vary from sample to sample, as the smaller gap in this sample is unlikely to be entirely attributable to migration over the second week in culture. There are also a few cells that appear to have migrated into the native tissue. Although the sparseness of these cells makes it difficult to assess the validity of this result, it is still a promising step in the right direction that good integration may be possible with these composite scaffolds. Growth factor treatments have also been used in previous studies in combination with enzyme pretreatments and have been shown to improve integration between neotissue and native tissue.[51] While a trypsin pretreatment was used in this work, specific growth factor treatments were not. This is a potential future direction to further improve integration between the repair tissue in the composite scaffold and the native cartilage.

Looking at all of the results collectively, it appears that the P:T-1 solid scaffold was the most successful of the four materials investigated in this study. The matrix production and accumulation was high, indicating that the cells in these composite scaffolds are motivated to produce cartilage-like matrix. The solid scaffold appears to fulfill its purpose of mechanically supporting the soft hydrogel at early time points to protect any early repair tissue formed and allow time for the cells to create a dense matrix. It is also bioabsorbable, allowing it to degrade and be cleared from the defect area once the cells have created enough matrix to make the repair tissue mechanically stable. This is preferable over the ePTFE materials, which are non-degradable and would be present for the remaining lifetime of the patient. The P:T-1 composite scaffolds also showed the potential for good integration with native tissue in cartilage defect model, although more robust and long-term experiments need to be done before determining long-term integration capabilities.
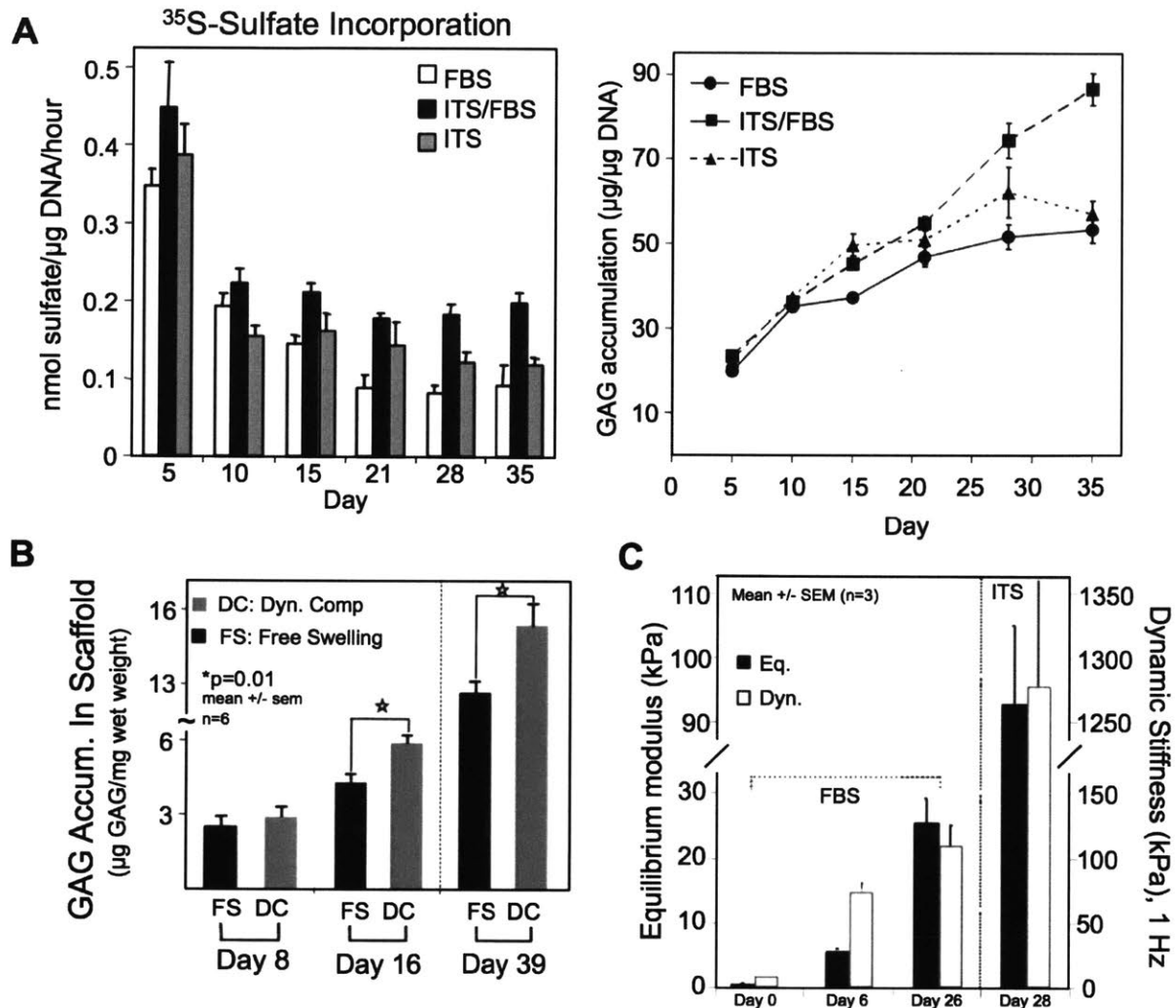
Figure 4.1: Previously published matrix production and mechanical properties of chondrocyte-seeded KLD hydrogels. (A) Sulfate incorporation and GAG accumulation in chondrocyte-seeded KLD hydrogels kept in 10% FBS medium, 0.2% FBS medium with 1% ITS, or 1% ITS medium, normalized to DNA content. GAG and DNA content measured by DMMB dye and Hoescht dye, respectively. Data published in [50]. (B) GAG accumulation in chondrocyte-seeded KLD hydrogels under alternate-day loading or free swelling, normalized by wet weight. Data published in [58]. (C) Mechanical properties of KLD hydrogels seeded with 15 million cells/mL and kept in 10% FBS medium, or KLD hydrogels seeded with 30 million cells/mL and kept in 0.2% FBS medium with 1% ITS. Samples were tested in uniaxial confined compression. Data published in [39].
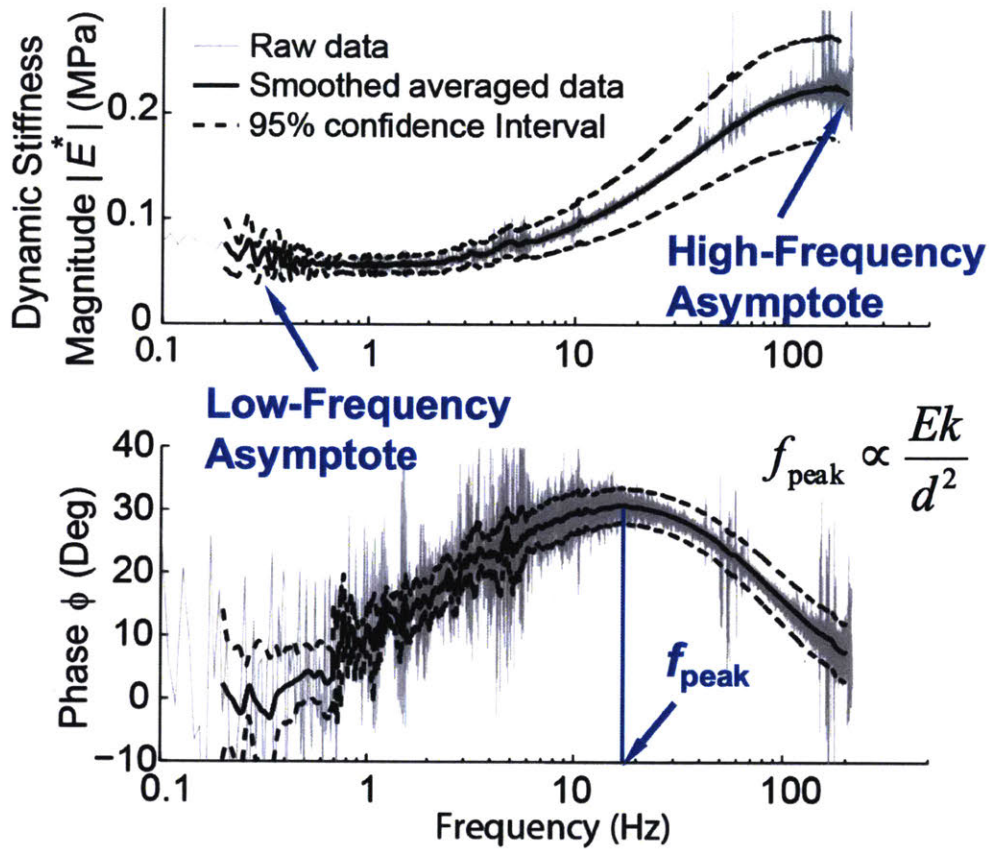
Figure 4.2: Dynamic modulus behavior in cartilage disks. Dynamic oscillatory indentation was performed by AFM at frequencies ranging from 0.1 to 100 Hz. The equation for f_{peak} is shown, where E is the equilibrium modulus, k the hydraulic permeability, and d the contact distance between the probe and the tissue, which was on the order of 10 μm for these data. Adapted from [55].

5. Conclusion

This work demonstrated the potential for composite scaffolds comprised of a bioabsorbable PGA:TMC solid scaffold loaded with a chondrocyte-seeded KLD hydrogel to be used for articular cartilage repair. This approach addresses key issues with both hydrogel and solid scaffold approaches, with the possibility of creating more robust tissue repair. While there is room for improvement in casting methods and potential to incorporate growth factor treatments and other pro-integrative components, this work has certainly been a first step in establishing these composite scaffolds as a promising candidate for tissue engineering new articular cartilage.

References

[1]   J. A. Buckwalter and H. J. Mankin, "Articular Cartilage - Tissue Design and Chondrocyte-Matrix Interactions," *The Journal of bone and joint surgery*. pp. 600–611, 1998.

[2]   N. Verzijl, J. DeGroot, S. R. Thorpe, R. A. Bank, J. N. Shaw, T. J. Lyons, J. W. J. Bijlsma, F. P. J. G. Lafeber, J. W. Baynes, and J. M. TeKoppele, "Effect of collagen turnover on the accumulation of advanced glycation end products," *J. Biol. Chem.*, vol. 275, no. 50, pp. 39027–39031, 2000.

[3]   P. J. Roughley and J. S. Mort, "The role of aggrecan in normal and osteoarthritic cartilage," *J. Exp. Orthop.*, vol. 1, no. 1, p. 8, 2014.

[4]   A. Maroudas, M. T. Bayliss, N. Uchitel-Kaushansky, R. Schneiderman, and E. Gilav, "Aggrecan turnover in human articular cartilage: use of aspartic acid racemization as a marker of molecular age.," *Arch. Biochem. Biophys.*, vol. 350, no. 1, pp. 61–71, 1998.

[5]   V. C. Mow, M. H. Holmes, and W. Michael Lai, "Fluid transport and mechanical properties of articular cartilage: A review," *J. Biomech.*, vol. 17, no. 5, pp. 377–394, 1984.

[6]   C. A. Poole, "Articular cartilage chondrons: form, function and failure.," *J. Anat.*, vol. 191 (Pt 1, pp. 1–13, 1997.

[7]   R. E. Wilusz, J. Sanchez-Adams, and F. Guilak, "The structure and function of the pericellular matrix of articular cartilage," *Matrix Biol.*, vol. 39, no. 5, pp. 25–32, Oct. 2014.

[8]   D. Correa and S. A. Lietman, "Articular cartilage repair: Current needs, methods and research directions," *Semin. Cell Dev. Biol.*, vol. 62, pp. 67–77, 2016.

[9]   E. B. Hunziker, L. C. Rosenberg, B. Y. E. B. Hunziker, M. D, L. C. Rosenberg, M. D, and N. E. W. York, "Repair of Partial-Thickness Defects in Articular Cartilage : Cell Recruitment from the Synovial Membrane *," *J. Bone Joint Surg. Am.*, vol. 78, no. 5, pp. 721–733, 1996.

[10]   C. P. Charalambous, "Cell origin and differentiation in the repair of full-thickness defects of articular cartilage," *Class. Pap. Orthop.*, pp. 377–379, 2014.

[11]   S. a Lietman, S. Miyamoto, P. R. Brown, N. Inoue, and a H. Reddi, "The temporal sequence of spontaneous repair of osteochondral defects in the knees of rabbits is dependent on the geometry of the defect.," *J. Bone Joint Surg. Br.*, vol. 84, no. 4, pp. 600–6, 2002.

[12]   E. J. Blain, S. J. Gilbert, R. J. Wardale, S. J. Capper, D. J. Mason, and V. C. Duance, "Up-Regulation of Matrix Metalloproteinase Expression and Activation Following Cyclical Compressive Loading of Articular Cartilage in Vitro," *Arch. Biochem. Biophys.*, vol. 396, no. 1, pp. 49–55, 2001.

[13]   G. D. Smith, G. Knutsen, and J. B. Richardson, "A clinical review of cartilage repair techniques," *J Bone Jt. Surg Am.*, vol. 87, no. 4, p. 715–24., 2005.

[14]   E. B. Hunziker, "Articular cartilage repair: Basic science and clinical progress. A review of the current status and prospects," *Osteoarthr. Cartil.*, vol. 10, no. 6, pp. 432–463, 2002.

[15]   P. C. Kreuz, M. R. Steinwachs, C. Erggelet, S. J. Krause, G. Konrad, M. Uhl, and N. Südkamp, "Results after microfracture of full-thickness chondral defects in different compartments in the knee," *Osteoarthr. Cartil.*, vol. 14, no. 11, pp. 1119–1125, 2006.

[16]   K. Mithoefer, T. McAdams, R. J. Williams, P. C. Kreuz, and B. R. Mandelbaum, "Clinical Efficacy of the Microfracture Technique for Articular Cartilage Repair in the Knee," *Am. J. Sports Med.*, vol. 37, no. 10, pp. 2053–2063, Oct. 2009.

[17] P. D. Benya and J. D. Shaffer, "Dedifferentiated chondrocytes reexpress the differentiated collagen phenotype when cultured in agarose gels," *Cell*, vol. 30, no. 1, pp. 215–224, 1982.

[18] M. Brittberg, A. Lindahl, A. Nilsson, C. Ohlsson, O. Isaksson, and L. Peterson, "Treatment of Deep Cartilage Defects in the Knee with Autologous Chondrocyte Transplantation," *N. Engl. J. Med.*, vol. 331, no. 14, pp. 889–895, Oct. 1994.

[19] G. A. Matricali, G. P. E. Dereymaeker, and F. P. Luvten, "Donor site morbidity after articular cartilage repair procedures: A review," *Acta Orthopaedica Belgica*, vol. 76, no. 5. pp. 669–674, 2010.

[20] S. Roberts, I. W. McCall, A. J. Darby, J. Menage, H. Evans, P. E. Harrison, and J. B. Richardson, "Autologous chondrocyte implantation for cartilage repair: monitoring its success by magnetic resonance imaging and histology," *Arthritis Res Ther*, vol. 5, no. 1, p. 1, 2002.

[21] W. Bartlett, J. A. Skinner, C. R. Gooding, R. W. J. Carrington, A. M. Flanagan, T. W. R. Briggs, and G. Bentley, "Autologous chondrocyte implantation versus matrix-induced autologous chondrocyte implantation for osteochondral defects of the knee: a prospective, randomised study.," *J. Bone Joint Surg. Br.*, vol. 87, no. 5, pp. 640–645, 2005.

[22] H. a Breinan, S. D. Martin, H. P. Hsu, and M. Spector, "Healing of canine articular cartilage defects treated with microfracture, a type-II collagen matrix, or cultured autologous chondrocytes.," *J. Orthop. Res.*, vol. 18, no. 5, pp. 781–789, 2000.

[23] H. A. Awad, M. Q. Wickham, H. A. Leddy, J. M. Gimble, and F. Guilak, "Chondrogenic differentiation of adipose-derived adult stem cells in agarose, alginate, and gelatin scaffolds," *Biomaterials*, vol. 25, no. 16, pp. 3211–3222, 2004.

[24] L. Bian, J. V. Fong, E. G. Lima, A. M. Stoker, G. a Ateshian, J. L. Cook, and C. T. Hung, "Dynamic Mechanical Loading Enhances Functional Properties of Tissue-Engineered Cartilage Using Mature Canine Chondrocytes," *Tissue Eng. Part A*, vol. 16, no. 5, pp. 1781–1790, May 2010.

[25] M. D. Buschmann, Y. A. Gluzband, A. J. Grodzinsky, J. H. Kimura, and E. B. Hunziker, "Chondrocytes in agarose culture synthesize a mechanically functional extracellular matrix," *J. Orthop. Res.*, vol. 10, no. 6, pp. 745–758, 1992.

[26] R. L. Mauck, M. a Soltz, C. C. Wang, D. D. Wong, P. H. Chao, W. B. Valhmu, C. T. Hung, and G. a Ateshian, "Functional tissue engineering of articular cartilage through dynamic loading of chondrocyte-seeded agarose gels.," *J. Biomech. Eng.*, vol. 122, no. 3, pp. 252–260, 2000.

[27] L. H. Christensen, "Host tissue interaction, fate, and risks of degradable and nondegradable gel fillers," *Dermatologic Surg.*, vol. 35, no. SUPPL. 2, pp. 1612–1619, 2009.

[28] A. J. Steward, Y. Liu, and D. R. Wagner, "Engineering cell attachments to scaffolds in cartilage tissue engineering," *Jom*, vol. 63, no. 4, pp. 74–82, 2011.

[29] J. T. Connelly, A. J. García, and M. E. Levenston, "Interactions between integrin ligand density and cytoskeletal integrity regulate BMSC chondrogenesis," *J. Cell. Physiol.*, vol. 217, no. 1, pp. 145–154, 2008.

[30] L. Q. Wan, J. Jiang, D. E. Arnold, X. E. Guo, H. H. Lu, and V. C. Mow, "Calcium Concentration Effects on the Mechanical and Biochemical Properties of Chondrocyte-Alginate Constructs.," *Cell. Mol. Bioeng.*, vol. 1, no. 1, pp. 93–102, 2008.

[31] H. J. Häuselmann, R. J. Fernandes, S. S. Mok, T. M. Schmid, J. a Block, M. B. Aydelotte,

K. E. Kuettner, and E. J. Thonar, "Phenotypic stability of bovine articular chondrocytes after long-term culture in alginate beads.," *J. Cell Sci.*, vol. 107, pp. 17–27, 1994.

[32] P. M. Ragan, V. I. Chin, H. H. Hung, K. Masuda, E. J. Thonar, E. C. Arner, a J. Grodzinsky, and J. D. Sandy, "Chondrocyte extracellular matrix synthesis and turnover are influenced by static compression in a new alginate disk culture system.," *Arch. Biochem. Biophys.*, vol. 383, no. 2, pp. 256–64, 2000.

[33] K. H. Bouhadir, K. Y. Lee, E. Alsberg, K. L. Damm, K. W. Anderson, and D. J. Mooney, "Degradation of partially oxidized alginate and its potential application for tissue engineering," *Biotechnol. Prog.*, vol. 17, no. 5, pp. 945–950, 2001.

[34] S. Zhang, T. C. Holmes, C. M. DiPersio, R. O. Hynes, X. Su, and A. Rich, "Self-complementary oligopeptide matrices support mammalian cell attachment," *Biomaterials*, vol. 16, no. 18, pp. 1385–1393, Dec. 1995.

[35] T. C. Holmes, "Novel peptide-based biomaterial scaffolds for tissue engineering," *Trends Biotechnol.*, vol. 20, no. 1, pp. 16–21, 2002.

[36] S. Zhang, T. Holmes, C. Lockshin, and a Rich, "Spontaneous assembly of a self-complementary oligopeptide to form a stable macroscopic membrane.," *Proc. Natl. Acad. Sci. U. S. A.*, vol. 90, no. 8, pp. 3334–3338, 1993.

[37] R. E. Miller, P. W. Kopesky, and A. J. Grodzinsky, "Growth factor delivery through self-assembling peptide scaffolds," *Clin. Orthop. Relat. Res.*, vol. 469, no. 10, pp. 2716–2724, 2011.

[38] P. W. Kopesky, E. J. Vanderploeg, J. S. Sandy, B. Kurz, and A. J. Grodzinsky, "Self-assembling peptide hydrogels modulate in vitro chondrogenesis of bovine bone marrow stromal cells.," *Tissue Eng. Part A*, vol. 16, no. 2, pp. 465–477, 2010.

[39] J. Kisiday, M. Jin, B. Kurz, H. Hung, C. Semino, S. Zhang, and a J. Grodzinsky, "Self-assembling peptide hydrogel fosters chondrocyte extracellular matrix production and cell division: Implications for cartilage tissue repair," *Proc. Natl. Acad. Sci.*, vol. 99, no. 15, pp. 9996–10001, 2002.

[40] R. E. Miller, A. J. Grodzinsky, E. J. Vanderploeg, C. Lee, D. J. Ferris, M. F. Barrett, J. D. Kisiday, and D. D. Frisbie, "Effect of self-assembling peptide, chondrogenic factors, and bone marrow-derived stromal cells on osteochondral repair," *Osteoarthr. Cartil.*, vol. 18, no. 12, pp. 1608–1619, Dec. 2010.

[41] C. Chih-Hung, L. Feng-Huei, K. Tzong-Fu, and H.-C. Liu, "Cartilage Tissue Engineering," *Biomed Eng Appl Basis Comm*, vol. 17, no. 2, pp. 61–71, 2005.

[42] J.-P. Chen, S.-F. Li, and Y.-P. Chiang, "Bioactive collagen-grafted poly-L-lactic acid nanofibrous membrane for cartilage tissue engineering.," *J. Nanosci. Nanotechnol.*, vol. 10, no. 8, pp. 5393–8, 2010.

[43] J. Suganuma and H. Alexander, "Biological response of intramedullary bone to poly-L-lactic acid," *J. Appl. Biomater.*, vol. 4, no. 1, pp. 13–27, 1993.

[44] K. Athanasiou, D. Korvick, and R. Schenck, "Biodegradable Implants for the Treatment of Osteochondral Defects in a Goat Model," *Tissue Eng.*, vol. 3, no. 4, pp. 363–373, 1997.

[45] W. J. C. M. Marijnissen, G. J. V. M. Van Osch, J. Aigner, S. W. Van Der Veen, A. P. Hollander, H. L. Verwoerd-Verhoef, and J. A. N. Verhaar, "Alginate as a chondrocyte-delivery substance in combination with a non-woven scaffold for cartilage tissue engineering," *Biomaterials*, vol. 23, no. 6, pp. 1511–1517, 2002.

[46] D. Hannouche, H. Terai, J. R. Fuchs, S. Terada, S. Zand, B. a Nasseri, H. Petite, L. Sedel, and J. P. Vacanti, "Engineering of implantable cartilaginous structures from bone marrow-

derived mesenchymal stem cells.," *Tissue Eng.*, vol. 13, no. 1, pp. 87–99, 2007.

[47]   L. Recha-Sancho, F. T. Moutos, J. Abell??, F. Guilak, and C. E. Semino, "Dedifferentiated human articular chondrocytes redifferentiate to a cartilage-like tissue phenotype in a poly("-caprolactone)/self-assembling peptide composite scaffold," *Materials (Basel).*, vol. 9, no. 6, 2016.

[48]   D. P. Mukherjee, D. F. Smith, S. H. Rogers, J. E. Emmanual, K. D. Jadin, and B. K. Hayes, "Effect of 3D-microstructure of bioabsorbable PGA:TMC scaffolds on the growth of chondrogenic cells," *J. Biomed. Mater. Res. - Part B Appl. Biomater.*, vol. 88, no. 1, pp. 92–102, 2009.

[49]   C. Co, M. K. Vickaryous, and T. G. Koch, "Membrane culture and reduced oxygen tension enhances cartilage matrix formation from equine cord blood mesenchymal stromal cells invitro," *Osteoarthr. Cartil.*, vol. 22, no. 3, pp. 472–480, 2014.

[50]   J. D. Kisiday, B. Kurz, M. a DiMicco, and A. J. Grodzinsky, "Evaluation of medium supplemented with insulin-transferrin-selenium for culture of primary bovine calf chondrocytes in three-dimensional hydrogel scaffolds.," *Tissue Eng.*, vol. 11, no. 1–2, pp. 141–151, 2005.

[51]   P. H. Liebesny, "Single-Dose Growth Factor Treatments to Enhance Cell Recruitment and Neotissue Integration in an Augmented Microfracture Cartilage Repair Model," Massachusetts Institute of Technology, 2016.

[52]   K. Chawla, K. Masuda, and R. L. Sah, "Tracking Chondrocytes and Assessing Their Proliferation with Carboxyfluorescein Diacetate Succinimidyl Ester: Effects on Cell Functions," *Tissue Eng. Part C Methods*, vol. 16, no. 2, pp. 301–310, Apr. 2010.

[53]   A. Wall and T. Board, "A direct spectrophotometric microassay for sulphated glycosaminoglycans in cartilage cultures," in *Classic Papers in Orthopaedics*, 2014, pp. 431–432.

[54]   V. L. Singer, L. J. Jones, S. T. Yue, and R. P. Haugland, "Characterization of PicoGreen reagent and development of a fluorescence-based solution assay for double-stranded DNA quantitation.," *Anal. Biochem.*, vol. 249, no. 2, pp. 228–238, 1997.

[55]   H. T. Nia, L. Han, Y. Li, C. Ortiz, and A. Grodzinsky, "Poroelasticity of cartilage at the nanoscale," *Biophys. J.*, vol. 101, no. 9, pp. 2304–2313, 2011.

[56]   H. T. Nia, I. S. Bozchalooi, Y. Li, L. Han, H. H. Hung, E. Frank, K. Youcef-Toumi, C. Ortiz, and A. Grodzinsky, "High-Bandwidth AFM-based rheology reveals that cartilage is most sensitive to high loading rates at early stages of impairment," *Biophys. J.*, vol. 104, no. 7, pp. 1529–1537, 2013.

[57]   C. W. Archer, S. Redman, I. Khan, J. Bishop, and K. Richardson, "Enhancing tissue integration in cartilage repair procedures," in *Journal of Anatomy*, 2006, vol. 209, no. 4, pp. 481–493.

[58]   J. D. Kisiday, M. Jin, M. A. DiMicco, B. Kurz, and A. J. Grodzinsky, "Effects of dynamic compressive loading on chondrocyte biosynthesis in self-assembling peptide scaffolds," *J. Biomech.*, vol. 37, no. 5, pp. 595–604, 2004.